Stress tensor in the linearized augmented plane wave method

Kamal Belbase,[1] Andreas Tröster,[2] and Peter Blaha[1]
[1]*Institute of Materials Chemistry, Vienna University of Technology, Getreidemarkt 9/165-TC, A-1060 Vienna, Austria*
[2]*Faculty of Physics, University of Vienna, Boltzmanngasse 5, A-1090 Vienna, Austria*

(Received 7 October 2021; accepted 10 November 2021; published 29 November 2021)

In this paper we present a detailed derivation of the stress tensor for the nonrelativistic full potential linearized augmented plane wave (LAPW) method. The formalism has been implemented into the WIEN2K code and has been thoroughly tested for the equilibrium lattice parameters in various solids. Hydrostatic and nonhydrostatic conditions have been applied and the accuracy of individual stress components has been tested at finite strain. We also tested the convergence of the stress tensor with respect to the basis set and found it necessary to increase the basis set a bit as compared to total energy calculations. The effect of the tetrahedron and Fermi-Dirac (FD) methods on the calculated stress is studied for aluminum and found that the FD method improves the results. Finally, a brief comparison with previous attempts in the literature on this topic is given.

DOI: 10.1103/PhysRevB.104.174113

I. INTRODUCTION

The minimization of the total energy (E_{tot}) with respect to the structural parameters of a material under a specific set of constraints is one of the fundamental tasks of modern solid state theory. Since in compounds with lower symmetry there could be tens to hundreds of structural parameters, determining the total energy alone is not sufficient for this goal and additional observables must be considered. One is the derivative of E_{tot} with respect to the atomic positions, i.e., the forces acting on the atoms [1–3]. Basically all major codes for solid state simulations have implemented efficient algorithms to determine these forces, and various force relaxation methods for optimizations of the atomic positions exist [4]. Another ingredient is knowledge of the stress tensor [5,6], i.e., the derivative of E_{tot} with respect to strain, which is necessary to optimize the lattice parameters and angles in low symmetry cases.

The stress tensor formalism was first adapted to density functional theory (DFT) [7,8] by Nielsen and Martin in Refs. [5,6], and verified using a plane wave based pseudopotential implementation. Their work was limited to the local density approximation (LDA), but later the derivation was extended to a semilocal exchange-correlation functional by Dal Corso and Resta [9]. A further extension to the projector augmented wave (PAW) method was published by Torrent *et al.* [10]. An alternative but less common way to calculate the stress tensor is via density functional perturbation theory (DFPT) [11], since strain may be regarded as a parametric perturbation. However, the application of strain also changes the periodic boundary conditions of the eigenfunctions of a Hamiltonian, which creates difficulties in the perturbative expansions used in DFPT [11]. These problems were finally overcome by an elegant reduced coordinate formulation in terms of strain-dependent metric tensors [12–14].

In plane wave pseudopotential calculations, a full structural optimization of both the atomic positions and the shape and size of the unit cell has thus been made possible and has been implemented in many such DFT codes. On the other hand, in all-electron linearized augmented plane wave (LAPW) methods [15,16], depending on the symmetry of the system at hand, a unit cell optimization could only be achieved by tedious if not prohibitively expensive procedures based on fitting lattice parameters to a possibly large number of total energy calculations, putting the all-electron LAPW approach at a significant disadvantage as compared to the pseudopotential plane wave based methods. Therefore, it is only too understandable that a number of efforts [17–21] have been made within the last two decades to remove this shortcoming of the LAPW approach. However, only the work of Nagasako and Oguchi [19,20] led to a fully functional stress tensor implementation, but their approach was based on the Soler-Williams LAPW method [22,23], which is somewhat different from standard LAPW. Thus it is fair to say that the task of implementing a fully functional stress tensor into a standard LAPW DFT code persisted to represent a long-standing and pressing problem. This task has finally been accomplished in our present paper.

Below, we shall present a thorough description of the formalism of the stress tensor within the LAPW method. The implementation into our WIEN2k code [24,25] is tested in terms of convergence and accuracy on a couple of examples. Then a brief comparison with previous respective work is given in the discussion. We limit ourselves to a nonrelativistic description of the valence states, while the core states can be handled fully relativistically.

II. STRESS TENSOR IN LAPW BASED METHODS

A. Basis function

The introduction of a set of basis functions is necessary to numerically solve Kohn-Sham single-particle equations in density functional theory (DFT) and to represent the electron density. In the LAPW method [16], the basis functions are defined according to the behavior of the potential and its effect on wave functions. Near the nuclei, the potential is very strong

but still approximately spherical, and the wave functions are similar to those of a free atom, and thus may contain several nodes and a cusp at the nucleus. In the so-called interstitial (IS) region farther away from the nuclei, the potential is weaker, and the wave functions are much smoother. Based on these observations, the unit cell of a crystal with volume Ω is divided into nonoverlapping atom-centered spheres with radii R_a and the remaining IS region. The LAPW basis functions are defined by smoothly augment plane waves $\frac{1}{\sqrt{\Omega}}e^{i(\boldsymbol{k}+\boldsymbol{K})\cdot\boldsymbol{r}}$ in the IS with an atomiclike angular momentum expansion in the atomic spheres, where $\boldsymbol{K}$ is a reciprocal lattice vector with modulus $|\boldsymbol{K}| \leqslant K_{\max}$ smaller than a chosen cutoff. Specifically, inside the atomic spheres around nucleus of an atom a at position $\boldsymbol{\tau}_a$, for each $l \leqslant l_{\max}$ we solve the radial Schrödinger equation using the spherically symmetric potential at certain prescribed energies E_l^a and obtain the resulting numerical solutions $u_l(r_a, E_l^a)$ and their energy derivatives $\dot{u}_l(r_a, E_l^a)$ as our radial basis functions:

$$\phi_{\boldsymbol{k}\boldsymbol{K}}(\boldsymbol{r}) = \begin{cases} \frac{1}{\sqrt{\Omega}} e^{i(\boldsymbol{k}+\boldsymbol{K})\cdot\boldsymbol{r}}, & \boldsymbol{r} \in \mathrm{IS}, \\ \sum_{l=0}^{l_{\max}} \sum_{m=-l}^{l} \left[a_{lm}^{a\boldsymbol{k}\boldsymbol{K}} u_l\left(r_a, E_l^a\right) + b_{lm}^{a\boldsymbol{k}\boldsymbol{K}} \dot{u}_l\left(r_a, E_l^a\right)\right] Y_{lm}(\hat{\boldsymbol{r}}_a), & \boldsymbol{r} \in R_a. \end{cases} \tag{1}$$

Here, $\boldsymbol{r}_a = \boldsymbol{r} - \boldsymbol{\tau}_a$ denotes the local position vector of a nucleus of an atom a with length $r_a = |\boldsymbol{r}_a|$ and directional unit vector $\hat{\boldsymbol{r}}_a = \boldsymbol{r}/r_a$, whereas the position vector $\boldsymbol{r}$ is defined with respect to the global coordinate system, which is often the crystal coordinate system. Y_{lm} is a spherical harmonic for angular momentum quantum numbers lm and $\boldsymbol{k}$ denotes a wave vector in the first Brillouin zone while $\boldsymbol{K}$ denotes a reciprocal lattice vector. In Eq. (1) each interstitial plane wave is augmented within the atomic spheres by a linear combination of radial functions plus their energy derivative times spherical harmonics. Imposing continuity in value and slope of the basis functions at the sphere boundary $r_a = R_a$ fixes the unknown coefficients $a_{lm}^{a\boldsymbol{k}\boldsymbol{K}}$ and $b_{lm}^{a\boldsymbol{k}\boldsymbol{K}}$ in Eq. (1).

In the presence of energetically high lying core states, which are often referred to as semicore states, the so-called local orbitals ϕ_{LO} (LOs) as described in Ref. [16] can be added. These additional functions contain an additional radial basis function at an energy $E_l^{a,\mathrm{sc}}$ close to the semicore (sc) eigenvalues and are nonzero only within the region of the atomic spheres.

The basis functions Eq. (1) and the LOs are used to represent the wave function $\psi_{\upsilon\boldsymbol{k}}(\boldsymbol{r})$ for the band υ and wave vector $\boldsymbol{k}$,

$$\psi_{\upsilon\boldsymbol{k}}^{\mathrm{v}}(\boldsymbol{r}) = \sum_{\boldsymbol{K}} c_{\upsilon\boldsymbol{k}\boldsymbol{K}} \phi_{\boldsymbol{k}\boldsymbol{K}}(\boldsymbol{r}) + \sum_{\mathbf{LO}} c_{\upsilon\boldsymbol{k},\mathrm{LO}} \phi_{\mathrm{LO}}(\boldsymbol{r}), \tag{2}$$

with expansion coefficients $c_{\upsilon\boldsymbol{k}\boldsymbol{K}}$ and $c_{\upsilon\boldsymbol{k},\mathrm{LO}}$, where the summation runs over all reciprocal lattice vectors with $|\boldsymbol{K}| \leqslant K_{\max}$ and all LOs of all atoms in the cell.

In the calculation of the total energy, the valence wave functions enter implicitly only through the valence charge density $\rho_{\mathrm{v}}(\boldsymbol{r}) = \sum_{\upsilon\boldsymbol{k}} n_{\upsilon\boldsymbol{k}} |\psi_{\upsilon\boldsymbol{k}}^{\mathrm{v}}(\boldsymbol{r})|^2$, where $n_{\upsilon\boldsymbol{k}}$ is the corresponding occupation number. When calculating the stress tensor, however, the individual wave functions are explicitly involved in the valence kinetic energy stress and the valence correction stress, as will be shown below.

The valence electron density is expanded into a Fourier series in the interstitial and into symmetry adapted lattice harmonics inside the spheres [16],

$$\rho_{\mathrm{v}}(\boldsymbol{r}) \equiv \begin{cases} \sum_{\boldsymbol{K}}^{G_{\max}} \rho(\boldsymbol{K}) e^{i(\boldsymbol{K})\cdot\boldsymbol{r}}, & \boldsymbol{r} \in \mathrm{IS}, \\ \sum_{\mathrm{LM}} \rho_{\mathrm{LM}}(r) Y_{\mathrm{LM}}(\hat{\boldsymbol{r}}), & \boldsymbol{r} \in R_a, \end{cases} \tag{3}$$

where $G_{\max}$ should be chosen at least as large as $2K_{\max}$. The total charge density and the potential are also expanded analogously to Eq. (3).

B. Stress tensor

The stress tensor is defined as the first-order variation in the total energy with respect to strain. The DFT Kohn-Sham total energy [26],

$$E_{\mathrm{tot}} = E_{\mathrm{kin}} + E_{\mathrm{es}} + E_{\mathrm{xc}}, \tag{4}$$

is therefore an appropriate starting point of its calculation. Here,

$$E_{\mathrm{kin}} = \sum_{\upsilon\boldsymbol{k}} n_{\upsilon\boldsymbol{k}} \epsilon_{\upsilon\boldsymbol{k}} - \int_{\Omega} d^3\boldsymbol{r}\, \rho(\boldsymbol{r}) V_{\mathrm{eff}}(\boldsymbol{r}), \tag{5a}$$

$$E_{\mathrm{es}} = \frac{1}{2}\int_{\Omega} d^3\boldsymbol{r}\, \rho(\boldsymbol{r}) V_C(\boldsymbol{r}) - \frac{1}{2}\sum_a Z_a V_M(\boldsymbol{\tau}_a), \tag{5b}$$

$$E_{\mathrm{xc}} = \int_{\Omega} d^3\boldsymbol{r}\, \rho(\boldsymbol{r}) \epsilon_{\mathrm{xc}}(\boldsymbol{r}), \tag{5c}$$

are the noninteracting kinetic, electrostatic, and exchange-correlation energy, respectively. $\epsilon_{\upsilon\boldsymbol{k}}$ represents the Kohn-Sham eigenvalue for the υth band at wave vector $\boldsymbol{k}$ and $V_{\mathrm{eff}}(\boldsymbol{r})$ is the effective potential, which is the sum of the Coulomb and the exchange-correlation potential $\mu_{\mathrm{xc}}(\rho)$. In (5b),

$$V_C(\boldsymbol{r}) = \int d^3\boldsymbol{r}' \frac{\rho(\boldsymbol{r}')}{|\boldsymbol{r} - \boldsymbol{r}'|} - \sum_a \frac{Z_a}{|\boldsymbol{r} - \boldsymbol{\tau}_a|}, \tag{6a}$$

$$V_M(\boldsymbol{\tau}_a) = \int d^3\boldsymbol{r}' \frac{\rho(\boldsymbol{r}')}{|\boldsymbol{r}' - \boldsymbol{\tau}_a|} - \sum_{a \neq b} \frac{Z_a}{|\boldsymbol{\tau}_a - \boldsymbol{\tau}_b|}, \tag{6b}$$

are the Coulomb and Madelung potential, respectively. Z_a is the nuclear charge of an atom a located at $\boldsymbol{\tau}_a$. In the local density approximation (LDA) the exchange-correlation energy per particle $\epsilon_{\mathrm{xc}}(\boldsymbol{r})$ is a local function of the total charge density ρ.

In order to compute the stress tensor, the total energy $E_{\mathrm{tot}}[\underline{\epsilon}]$ of a strained system needs to be differentiated with

respect to the strain tensor components $\epsilon_{\alpha\beta}$:

$$\sigma_{\alpha\beta} = \frac{1}{\Omega}\frac{dE_{\text{tot}}[\underline{\underline{\epsilon}}]}{d\epsilon_{\alpha\beta}}\bigg|_{\underline{\underline{\epsilon}}=0}. \tag{7}$$

The symbol $[\underline{\underline{\epsilon}}]$ will be generally used to denote quantities after deformation. Greek letters α and β are used to denote the Cartesian coordinate components. The substitution of Eq. (4) in Eq. (7) suggests that in order to calculate the stress tensor, the strain variation of E_{kin}, E_{es}, and E_{xc} must first be assessed, which is done in the following sections.

1. The strain variation of the kinetic energy

This contribution results from the change in kinetic energy upon deforming the system. Formally, $E_{\text{kin}}[\underline{\underline{\epsilon}}]$ is given by Eq. (5a) evaluated in the strained system. Taking the strain derivative of $E_{\text{kin}}[\underline{\underline{\epsilon}}]$ results in

$$\frac{dE_{\text{kin}}[\underline{\underline{\epsilon}}]}{d\epsilon_{\alpha\beta}}\bigg|_{\underline{\underline{\epsilon}}=0} = \frac{d}{d\epsilon_{\alpha\beta}}\bigg|_{\underline{\underline{\epsilon}}=0}\sum_{\upsilon\boldsymbol{k}_{[\underline{\underline{\epsilon}}]}} n_{\upsilon\boldsymbol{k}[\underline{\underline{\epsilon}}]}[\underline{\underline{\epsilon}}]\epsilon_{\upsilon\boldsymbol{k}[\underline{\underline{\epsilon}}]}[\underline{\underline{\epsilon}}] - \frac{d}{d\epsilon_{\alpha\beta}}\bigg|_{\underline{\underline{\epsilon}}=0}\int_{\Omega[\underline{\underline{\epsilon}}]} d^3\boldsymbol{r}_\epsilon\,\rho[\underline{\underline{\epsilon}}](\boldsymbol{r}_\epsilon)V_{\text{eff}}[\underline{\underline{\epsilon}}](\boldsymbol{r}_\epsilon). \tag{8}$$

To calculate the first term, the strain derivative of the occupation number is required. In parallel with the calculation of LAPW forces [3], we assume that the strain dependence of the occupation numbers $n_{\upsilon\boldsymbol{k}[\underline{\underline{\epsilon}}]}[\underline{\underline{\epsilon}}]$ vanishes to linear order, i.e., $\frac{dn_{\upsilon\boldsymbol{k}[\underline{\underline{\epsilon}}]}[\underline{\underline{\epsilon}}]}{d\epsilon_{\alpha\beta}}|_{\underline{\underline{\epsilon}}=0} \to 0$. The strain variation of the total Kohn-Sham eigenvalues $\frac{d\epsilon_{\upsilon\boldsymbol{k}[\underline{\underline{\epsilon}}]}[\underline{\underline{\epsilon}}]}{d\epsilon_{\alpha\beta}}|_{\underline{\underline{\epsilon}}=0}$ is split into the change of core eigenvalues $\frac{d\epsilon^{\text{c}}[\underline{\underline{\epsilon}}]}{d\epsilon_{\alpha\beta}}|_{\underline{\underline{\epsilon}}=0}$ and valence eigenvalues $\frac{d\epsilon^{\text{v}}_{\upsilon\boldsymbol{k}[\underline{\underline{\epsilon}}]}[\underline{\underline{\epsilon}}]}{d\epsilon_{\alpha\beta}}|_{\underline{\underline{\epsilon}}=0}$. We first calculate the strain variation of the core eigenvalues using the Hellmann-Feynman theorem similar to the strategy used in the LAPW force calculations:

$$\begin{aligned}\sum_c n_c\frac{d\epsilon^c[\underline{\underline{\epsilon}}]}{d\epsilon_{\alpha\beta}}\bigg|_{\underline{\underline{\epsilon}}=0} &= \sum_c n_c\frac{d}{d\epsilon_{\alpha\beta}}\left\langle\psi^a_c[\underline{\underline{\epsilon}}](\boldsymbol{r}_\epsilon)\,|\,-\frac{1}{2}\nabla[\underline{\underline{\epsilon}}]^2 + V_{\text{eff}}[\underline{\underline{\epsilon}}](\boldsymbol{r}_\epsilon)\,|\,\psi^a_c[\underline{\underline{\epsilon}}](\boldsymbol{r}_\epsilon)\right\rangle\bigg|_{\underline{\underline{\epsilon}}=0}\\ &= \sum_{a\in\Omega}\int_{R_a} d^3r_a\rho^a_c(\boldsymbol{r}_a)\frac{dV_{\text{eff}}[\underline{\underline{\epsilon}}](\boldsymbol{r}_a)}{d\epsilon_{\alpha\beta}}\bigg|_{\underline{\underline{\epsilon}}=0}.\end{aligned} \tag{9}$$

Here, $\psi^a_c(\boldsymbol{r})$ denotes a core state c of an atom a, $\langle\cdot\,|\,\cdot\,|\,\cdot\rangle$ refers to the volume integration within the unit cell, the sum $\sum_{a\in\Omega}$ runs over all atoms and core states of the unit cell, ρ^a_c refers to the core electron density of an atom a, and $\int_{R_a} d^3r_a$ indicates that the integration is limited to atomic spheres because the core wave functions vanish outside the spheres.

In the following we evaluate the strain variation of the valence eigenvalues,

$$\frac{d\epsilon^{\text{v}}_{\upsilon\boldsymbol{k}[\underline{\underline{\epsilon}}]}}{d\epsilon_{\alpha\beta}} = \frac{d}{d\epsilon_{\alpha\beta}}\frac{\int_{\Omega[\underline{\underline{\epsilon}}]} d^3r_\epsilon\,\psi^{\text{v}*}_{\upsilon\boldsymbol{k}[\underline{\underline{\epsilon}}]}[\underline{\underline{\epsilon}}](\boldsymbol{r}_\epsilon)\widehat{H}_{\text{eff}}[\underline{\underline{\epsilon}}](\boldsymbol{r}_\epsilon)\psi^{\text{v}}_{\upsilon\boldsymbol{k}[\underline{\underline{\epsilon}}]}[\underline{\underline{\epsilon}}](\boldsymbol{r}_\epsilon)}{\int_{\Omega[\underline{\underline{\epsilon}}]} d^3r_\epsilon\,\psi^{\text{v}*}_{\upsilon\boldsymbol{k}[\underline{\underline{\epsilon}}]}[\underline{\underline{\epsilon}}](\boldsymbol{r}_\epsilon)\psi^{\text{v}}_{\upsilon\boldsymbol{k}[\underline{\underline{\epsilon}}]}[\underline{\underline{\epsilon}}](\boldsymbol{r}_\epsilon)}. \tag{10}$$

(1) The volume integration is transformed back to the unstrained unit cell as $\int_{\Omega[\underline{\underline{\epsilon}}]} d^3\boldsymbol{r}_\epsilon \to \det(\underline{\underline{1}}+\underline{\underline{\epsilon}})\int_\Omega d^3\boldsymbol{r}$.

(2) Differentiation with respect to the strain is simplified as described in Appendix B.

(3) The strain variation of the effective Hamiltonian is computed as

$$\frac{dH_{\text{eff}}[\underline{\underline{\epsilon}}](\boldsymbol{r}[\underline{\underline{\epsilon}}])}{d\epsilon_{\alpha\beta}}\bigg|_{\underline{\underline{\epsilon}}=0} = \frac{1}{2}(\partial_\alpha\partial_\beta + \partial_\beta\partial_\alpha) + \frac{dV_{\text{eff}}[\underline{\underline{\epsilon}}](\boldsymbol{r}[\underline{\underline{\epsilon}}])}{d\epsilon_{\alpha\beta}}\bigg|_{\underline{\underline{\epsilon}}=0}. \tag{11}$$

The first term results from the strain variation of the nonrelativistic kinetic energy $\frac{d\nabla^2[\underline{\underline{\epsilon}}]}{d\epsilon_{\alpha\beta}}$ of the Hamiltonian operator and the second term results from a change in the total potential according to the strain. The symbol $\partial_\alpha = \hat{\boldsymbol{r}}_\alpha\frac{\partial}{\partial r}$ is shorthand for the partial derivative along the Cartesian direction α.

Using Eq. (11) and Appendix B, Eq. (10) can be brought into the form

$$\begin{aligned}\frac{d\epsilon^{\text{v}}_{\upsilon\boldsymbol{k}[\underline{\underline{\epsilon}}]}}{d\epsilon_{\alpha\beta}} &= 2\,\text{Re}\left\langle\frac{d\psi^{\text{v}}_{\upsilon\boldsymbol{k}[\underline{\underline{\epsilon}}]}[\underline{\underline{\epsilon}}](\boldsymbol{r}[\underline{\underline{\epsilon}}])}{d\epsilon_{\alpha\beta}}\bigg|_{\underline{\underline{\epsilon}}=0}\,\Big|\,\widehat{H}_{\text{eff}}(\boldsymbol{r}) - \epsilon^{\text{v}}_{\upsilon\boldsymbol{k}}\,\Big|\,\psi^{\text{v}}_{\upsilon\boldsymbol{k}}(\boldsymbol{r})\right\rangle + \frac{1}{2}\int_\Omega d^3r\,\psi^{\text{v}}_{\upsilon\boldsymbol{k}}(\boldsymbol{r})(\partial_\alpha\partial_\beta+\partial_\beta\partial_\alpha)\psi^{\text{v}}_{\upsilon\boldsymbol{k}}(\boldsymbol{r})\\ &\quad + \int_\Omega d^3r\,\rho_{\text{v}}(\boldsymbol{r})\frac{dV_{\text{eff}}[\underline{\underline{\epsilon}}](\boldsymbol{r}[\underline{\underline{\epsilon}}])}{d\epsilon_{\alpha\beta}}\bigg|_{\underline{\underline{\epsilon}}=0}.\end{aligned} \tag{12}$$

Here, Re denotes the real part of a complex number. The first term of Eq. (12), which is similar to the Pulay term in the force calculation, is the so-called valence correction or incomplete basis-set (IBS) correction. To compute this IBS correction, the valence states described in Eq. (2) need to be defined in the strained environment followed by differentiation with respect to the

strain:

$$\left.\frac{d\psi^{\mathrm{v}}_{v\boldsymbol{k}[\underline{\underline{\epsilon}}]}(\boldsymbol{r}[\underline{\underline{\epsilon}}])}{d\epsilon_{\alpha\beta}}\right|_{\underline{\underline{\epsilon}}=0} = \sum_{\boldsymbol{K}}\left(\frac{d}{d\epsilon_{\alpha\beta}}\left[\frac{c_{v\boldsymbol{k}[\underline{\underline{\epsilon}}]\boldsymbol{K}[\underline{\underline{\epsilon}}]}[\underline{\underline{\epsilon}}]}{\sqrt{\Omega[\underline{\underline{\epsilon}}]}}\right]_{\underline{\underline{\epsilon}}=0}\sqrt{\Omega}\phi_{\boldsymbol{k}\boldsymbol{K}}(\boldsymbol{r}) + \frac{c_{v\boldsymbol{k}\boldsymbol{K}}}{\sqrt{\Omega}}\frac{d}{d\epsilon_{\alpha\beta}}\left[\sqrt{\Omega[\underline{\underline{\epsilon}}]}\phi_{\boldsymbol{k}[\underline{\underline{\epsilon}}]\boldsymbol{K}[\underline{\underline{\epsilon}}]}[\underline{\underline{\epsilon}}](\boldsymbol{r}[\underline{\underline{\epsilon}}])\right]_{\underline{\underline{\epsilon}}=0}\right). \tag{13}$$

(1) The first term on the right-hand side of (13) is proportional to the basis functions, so it does not contribute to the valence correction at all.

(2) The second term does not contribute in the interstitial region since the Ω times the basis function do not change with strain in first order [see Eq. (D1) of Appendix D]. Therefore, it suffices to calculate the total integral $\langle\cdot|\cdot|\cdot\rangle$ only within the atomic spheres $\langle\cdot|\cdot|\cdot\rangle^{R_a}$. Inside the atomic spheres, using the so-called *frozen augmentation approximation* [3], we discard an explicit strain dependency in $\phi_{\boldsymbol{k}[\underline{\underline{\epsilon}}]\boldsymbol{K}[\underline{\underline{\epsilon}}]}[\underline{\underline{\epsilon}}](\boldsymbol{r}[\underline{\underline{\epsilon}}])$ while keeping an implicit dependency via its smeared argument, i.e., $\phi_{\boldsymbol{k}[\underline{\underline{\epsilon}}]\boldsymbol{K}[\underline{\underline{\epsilon}}]}[\underline{\underline{\epsilon}}](\boldsymbol{r}[\underline{\underline{\epsilon}}]) \to \phi_{\boldsymbol{k}[\underline{\underline{\epsilon}}]\boldsymbol{K}[\underline{\underline{\epsilon}}]}(\boldsymbol{r}[\underline{\underline{\epsilon}}])$ [see Eq. (D6)].

Substitution of Eqs. (9) and (12) into (8), and the evaluation of the second integral of Eq. (8) along the lines of Appendix B, results in

$$\begin{aligned}\left.\frac{dE_{\mathrm{kin}}[\underline{\underline{\epsilon}}]}{d\epsilon_{\alpha\beta}}\right|_{\underline{\underline{\epsilon}}=0} &= 2\sum_{v\boldsymbol{k}} n_{v\boldsymbol{k}}\,\mathrm{Re}\left\langle\left.\frac{d\psi^{\mathrm{v}}_{v\boldsymbol{k}[\underline{\underline{\epsilon}}]}(\boldsymbol{r}[\underline{\underline{\epsilon}}])}{d\epsilon_{\alpha\beta}}\right|_{\underline{\underline{\epsilon}}=0}\middle|\,\widehat{H}_{\mathrm{eff}}(\boldsymbol{r}) - \epsilon_{v\boldsymbol{k}}\,\middle|\,\psi^{\mathrm{v}}_{v\boldsymbol{k}}\right\rangle^{R_a} + \frac{1}{2}\sum_{v\boldsymbol{k}} n_{v\boldsymbol{k}}\int_\Omega d^3r\,\psi^{\mathrm{v}*}_{v\boldsymbol{k}}(\boldsymbol{r})(\partial_\alpha\partial_\beta + \partial_\beta\partial_\alpha)\psi^{\mathrm{v}}_{v\boldsymbol{k}}(\boldsymbol{r})\\ &\quad -\delta_{\alpha\beta}\int_\Omega d^3r\,\rho(\boldsymbol{r})V_{\mathrm{eff}}(\boldsymbol{r}) - \int_\Omega d^3r\frac{d\rho[\underline{\underline{\epsilon}}](\boldsymbol{r}[\underline{\underline{\epsilon}}])}{d\epsilon_{\alpha\beta}}V_{\mathrm{eff}}(\boldsymbol{r}) - \frac{1}{2}\sum_{a\in\Omega}\int_{R_a} d^3r_a\rho^a_c(\boldsymbol{r}_a)(r_\beta\partial_\alpha + r_\alpha\partial_\beta)V_{\mathrm{eff}}(\boldsymbol{r}).\end{aligned} \tag{14}$$

The evaluation of the above integrals is straightforward:

(1) Integrals over the unit cell are divided into integrals over atomic spheres and over the interstitial region.

(2) The first and second terms can be simplified using Eq. (D3) and Eqs. (C1) and (C9), respectively.

(3) The third term is easy to evaluate using the corresponding expressions for $\rho(\boldsymbol{r})$ and $V_{\mathrm{eff}}(\boldsymbol{r})$ in terms of the spherical harmonics expansion inside atomic spheres and the Fourier expansion in the interstitial region.

(4) The fourth term will get canceled in combination with similar terms appearing in the electrostatic and exchange-correlation stress, and hence does not contribute to the final stress tensor.

(5) The last term is referred to as the core correction stress. When the unit cell is deformed, the core states change in two different ways. On the one hand, the core states will move along with the nuclei to a new position in the strained unit cell. On the other hand, the total potential in the unit cell is changed, and core states will interact with this modified potential. The explicit expression of the core correction in Eq. (14) illustrates that the core correction resembles the latter change. For a detailed evaluation, see Appendix E.

2. Strain variation of electrostatic energy

This contribution results from the change in electrostatic energy according to strain. In the following the electrostatic energy given in Eq. (5b) is first formulated in the strained system, i.e., $E_{\mathrm{es}}[\underline{\underline{\epsilon}}]$, and then differentiated with respect to strain:

$$\begin{aligned}\left.\frac{dE_{\mathrm{es}}[\underline{\underline{\epsilon}}]}{d\epsilon_{\alpha\beta}}\right|_{\underline{\underline{\epsilon}}=0} &= \frac{1}{2}\left.\frac{d}{d\epsilon_{\alpha\beta}}\right|_{\underline{\underline{\epsilon}}=0}\int_{\Omega[\underline{\underline{\epsilon}}]} d^3r_\epsilon\,\rho[\underline{\underline{\epsilon}}](\boldsymbol{r}_\epsilon)V_C[\underline{\underline{\epsilon}}](\boldsymbol{r}_\epsilon)\\ &\quad -\frac{1}{2}\sum_{a\in\Omega[\underline{\underline{\epsilon}}]} Z_a\left.\frac{dV_M[\underline{\underline{\epsilon}}](\boldsymbol{\tau}_a[\underline{\underline{\epsilon}}])}{d\epsilon_{\alpha\beta}}\right|_{\underline{\underline{\epsilon}}=0}.\end{aligned} \tag{15}$$

Using Eq. (B1) to evaluate the strained variation of the integral, we obtain $\sigma^{\mathrm{es}}_{\alpha\beta}$ as

$$\begin{aligned}\left.\frac{dE_{\mathrm{es}}[\underline{\underline{\epsilon}}]}{d\epsilon_{\alpha\beta}}\right|_{\underline{\underline{\epsilon}}=0} &= \frac{\delta_{\alpha\beta}}{2}\int_\Omega d^3r\,\rho(\boldsymbol{r})V_C(\boldsymbol{r})\\ &\quad + \int_\Omega d^3r\left.\frac{d\rho[\underline{\underline{\epsilon}}](\boldsymbol{r}[\underline{\underline{\epsilon}}])}{d\epsilon_{\alpha\beta}}\right|_{\underline{\underline{\epsilon}}=0} V_C(\boldsymbol{r})\\ &\quad + \frac{1}{2}\int_\Omega d^3r\,\rho(\boldsymbol{r})\left.\frac{dV_C[\underline{\underline{\epsilon}}](\boldsymbol{r}[\underline{\underline{\epsilon}}])}{\epsilon_{\alpha\beta}}\right|_{\underline{\underline{\epsilon}}=0}\\ &\quad -\frac{1}{2}\sum_{a\in\Omega} Z_a\left.\frac{dV_M[\underline{\underline{\epsilon}}](\boldsymbol{\tau}_a[\underline{\underline{\epsilon}}])}{d\epsilon_{\alpha\beta}}\right|_{\underline{\underline{\epsilon}}=0},\end{aligned} \tag{16}$$

where $\delta_{\alpha\beta}$ denotes the Kronecker delta.

(1) The first term contributes only to the diagonal elements of $\sigma^{es}_{\alpha\beta}$. The corresponding integral is straightforward to obtain.

(2) The second term cancels with a corresponding term in Eq. (14).

(3) When calculating the strain variation of $V_C(\boldsymbol{r})$ and $V_M(\boldsymbol{r})$, the strained charge density $\rho[\underline{\underline{\epsilon}}](\boldsymbol{r}[\underline{\underline{\epsilon}}])$ is replaced by the charge density of the unstrained system but smeared over the strained system, i.e., $\rho((\underline{\underline{1}} - \underline{\underline{\epsilon}})\boldsymbol{r}_\epsilon)$.

It is clear from the above equation that to evaluate the electrostatic stress tensor we need to calculate the strain variation of the Coulomb and Madelung potentials. Two different approaches are available in Refs. [17,21] to calculate the change in the potential under infinitesimal strain, but due to the lack of sufficient results it is unclear which approach works best for the original LAPW method. In Ref. [17], the authors suggest that the strain potential can be determined directly from the strained charge density using Poisson's equation. In contrast, in Ref. [21] an explicit derivation of the strain variation of the Coulomb potential using Weinert's method

[27] was presented. We tried to work with the expression provided in Ref. [21] first, but unfortunately this resulted in huge errors in the calculated stress tensor and we could not figure out where the problem was actually originating from. Similar problems are reported by Klüppelberg in Ref. [21]. Therefore, after some painstaking numerical testing we finally decided to resort to a different approach to simplify the electrostatic stress tensor. In our derivation we first transform all the integrals from the strained to the unstrained system. Following the standard procedure of the LAPW method, the total integral is divided into the interstitial and the atomic sphere parts. When solving the strain variation of the Coulomb potential in the interstitial, we assume that the Fourier component of both the real interstitial charge density and the pseudocharge density are invariant under strain [see Eqs. (F3) and (F4)], and that the change in the potential is only due to the change in the reciprocal lattice vector. This leads to our expression of the electrostatic stress tensor in the interstitial region similar to that in Refs. [5,19]. In the atomic sphere region, we only consider the change in $V_C(\boldsymbol{r})$ due to the change in the unit cell volume and the change in the radial vector.

3. The strain variation of the exchange-correlation energy

The LDA exchange-correlation energy per particle $\epsilon_{\rm xc}(\rho)$ depends exclusively on the density ρ. When the system is deformed, $E_{\rm xc}$ changes compared to the undeformed system, which makes it necessary to evaluate the strain variation of $E_{\rm xc}$. In the following, $E_{\rm xc}$ given in Eq. (5c) is first defined in the strained system $E_{\rm xc}[\underline{\underline{\epsilon}}]$, differentiated with respect to strain and using the same techniques discussed in the calculation of the kinetic energy and the electrostatic stress tensor results in

$$\left.\frac{dE_{\rm xc}[\underline{\underline{\epsilon}}]}{d\epsilon_{\alpha\beta}}\right|_{\underline{\underline{\epsilon}}=0} = \delta_{\alpha\beta}\int_\Omega d^3r\,\rho(\boldsymbol{r})\epsilon_{\rm xc} + \int_\Omega d^3r\,\frac{d\rho[\underline{\underline{\epsilon}}](\boldsymbol{r}[\underline{\underline{\epsilon}}])}{d\epsilon_{\alpha\beta}}\mu_{\rm xc}. \tag{17}$$

Due to the presence of the Kronecker delta, the first term only contributes to the diagonal elements of $\sigma^{\rm xc}_{\alpha\beta}$. The second term cancels with a corresponding contribution in the double counting part of the kinetic energy—the second term of Eq. (5a). In the spin-polarized case, contributions of spin-up and spin-down charge densities must be explicitly included, yielding separate contributions to the total exchange-correlation stress tensor.

4. Total stress tensor

We collect the strain variation of the kinetic energy, the electrostatic energy, and the exchange-correlation energy from Eqs. (14), (16), and (17) to define the strain variation of the total energy and thereby the stress tensor, Eq. (7). Finally the stress tensor in the LAPW method is

$$\sigma_{\alpha\beta} = \sigma^{\rm val,kin}_{\alpha\beta} + \sigma^{\rm val,corr}_{\alpha\beta} + \sigma^{\rm core,corr}_{\alpha\beta} + \sigma^{\rm es}_{\alpha\beta} + \sigma^{\rm xc,LDA}_{\alpha\beta}, \tag{18}$$

with

$$\sigma^{\rm val,kin}_{\alpha\beta} = \frac{1}{2\Omega}\sum_{\upsilon\boldsymbol{k}} n_{\upsilon\boldsymbol{k}}\int_\Omega d^3r\,\psi^{\rm v*}_{\upsilon\boldsymbol{k}}(\boldsymbol{r})(\partial_\alpha\partial_\beta + \partial_\beta\partial_\alpha)\psi^{\rm v}_{\upsilon\boldsymbol{k}}(\boldsymbol{r}), \tag{19}$$

$$\sigma^{\rm val,corr}_{\alpha\beta} = \frac{2}{\Omega}\sum_{\upsilon\boldsymbol{k}} n_{\upsilon\boldsymbol{k}}\,{\rm Re}\left\langle \left.\frac{d\psi^{\rm v}_{\upsilon\boldsymbol{k}[\underline{\underline{\epsilon}}]}(\boldsymbol{r}[\underline{\underline{\epsilon}}])}{d\epsilon_{\alpha\beta}}\right|_{\underline{\underline{\epsilon}}=0} \middle| \,\widehat{H}_{\rm eff}(\boldsymbol{r}) - \epsilon_{\upsilon\boldsymbol{k}} \,\middle|\, \psi^{\rm v}_{\upsilon\boldsymbol{k}}\right\rangle^{R_a}, \tag{20}$$

$$\sigma^{\rm core,corr}_{\alpha\beta} = -\frac{1}{2\Omega}\sum_{a\in\Omega}\int_{R_a} d^3r\,\rho^a_c(\boldsymbol{r})(r_\beta\partial_\alpha + r_\alpha\partial_\beta)V_{\rm eff}(\boldsymbol{r}), \tag{21}$$

$$\sigma^{\rm es}_{\alpha\beta} = -\frac{\delta_{\alpha\beta}}{2}\int_\Omega d^3\boldsymbol{r}\rho(\boldsymbol{r})V_C(\boldsymbol{r}) + \frac{1}{2}\int_\Omega d^3\boldsymbol{r}\rho(\boldsymbol{r})\left.\frac{dV_C[\underline{\underline{\epsilon}}](\boldsymbol{r}[\underline{\underline{\epsilon}}])}{\epsilon_{\alpha\beta}}\right|_{\underline{\underline{\epsilon}}=0} - \frac{1}{2}\sum_{a\in\Omega} Z_a\frac{d}{d\epsilon_{\alpha\beta}}V_M[\underline{\underline{\epsilon}}](\boldsymbol{\tau}_a[\underline{\underline{\epsilon}}])\Big|_{\underline{\underline{\epsilon}}=0}, \tag{22}$$

$$\sigma^{\rm xc,LDA}_{\alpha\beta} = \delta_{\alpha\beta}\int_\Omega d^3r\,\rho(\boldsymbol{r})[\epsilon_{\rm xc}(\rho) - \mu_{\rm xc}(\rho)]. \tag{23}$$

The final expressions of Eqs. (19)–(23), which are implemented in the WIEN2K code, may be found in Appendix G, and the results for validating our implementation are presented in Sec. III. Note that most of the quantities such as $\psi_{\upsilon\boldsymbol{k}}(\boldsymbol{r})$, $\rho(\boldsymbol{r})$, $\rho_c(\boldsymbol{r}_a)$, $V_C(\boldsymbol{r})$, $\epsilon_{\rm xc}$, $\mu_{\rm xc}$, and $\partial\epsilon_{\rm xc}/\partial\sigma$ that appear in this formula are readily available from a regular total energy calculation. Most of the terms involved in Eqs. (19)–(23) are easy to evaluate, but the evaluation of $\sigma^{\rm val,corr}_{\alpha\beta}$ and $\sigma^{\rm val,kin}_{\alpha\beta}$, which explicitly contains the wave functions, is both mathematically and computationally demanding.

III. RESULTS

In the LAPW method, the accuracy of results is controlled by the selection of various input parameters. One of them is $R_aK_{\rm max}$, where R_a is the smallest atomic sphere size among the constituent atoms, and $K_{\rm max}$ is the modulus of the largest reciprocal vector contributing to the Fourier expansion of wave functions. $R_aK_{\rm max}$ limits the total number of basis functions in the LAPW method and determines the cutoff energy of the plane waves via $E_{\rm max} = K^2_{\rm max}$. The value of $R_aK_{\rm max}$ in a total energy calculation typically ranges from 7 to 10 depending on the atoms in the system (for elements with f electrons even a value of 11 may be required). However, it is unclear how the accuracy of the analytically computed stress tensor would depend on the choice of $R_aK_{\rm max}$. One may anticipate that a larger value than for regular total energy calculations might be required, because the energy is variational with respect to small changes in the density according to the

Hohenberg-Kohn theorems [7,8] and thus errors in the density only enter in quadratic order, while there is no corresponding variational principle for the stress tensor so that errors may already manifest themselves in linear order.

In addition to $R_aK_{\max}$, $l_{\max}$, the cutoff value for the expansion of basis functions in the region of the atomic spheres, the cutoff value $G_{\max}$ for the plane wave expansion of the charge densities and the potential, the cutoff value $L_{\max}^{\text{ns}}$ for the expansion of the nonspherical potential, and the chosen size of the k mesh in the Brillouin zone (BZ) also have a certain impact on the accuracy of the calculation. Moreover, in metallic systems, the choice of the smearing method and, if the Fermi-Dirac (FD) method is chosen, the particular value of the corresponding temperature broadening parameter, determine the quality of results.

In the sections below we provide various convergence tests of the above mentioned parameters on several systems. The results were produced using our WIEN2K [24,25] implementation using LDA for the exchange-correlation energy and potential. To validate our implementation, we compare the results of the stress tensor with the least squares fit of total energy versus volume using the Birch-Murnaghan [28] (BM) equation of state. From the BM fit we obtain the pressure $P^{(E)} := -\frac{dE(\Omega)}{d\Omega}$ [see Fig. 1(a)]. The resulting pressures $P^{(E)}$ are then compared with the hydrostatic pressure $P^{(\sigma)} := -(\sigma_{11}+\sigma_{22}+\sigma_{33})/3$ as calculated directly from our analytical expression Eq. (18) of the stress tensor. The difference between $P^{(E)}$ and $P^{(\sigma)}$ represents an excellent measure of the accuracy and reliability of our formalism. In particular, a small remainder of $P^{(E)} - P^{(\sigma)}$ within some acceptable limit suggests that the zero pressure equilibrium configuration predicted from the stress tensor calculation is quite close to that obtained from the minimum of the total energy.

A. Aluminum

For fcc aluminum, the total energy and $P^{(E)}$ as a function of Ω for different $R_aK_{\max}$ is plotted in Fig. 1(a). $P^{(\sigma)}$ is shown in Fig. 1(b), and the deviation $P^{(E)} - P^{(\sigma)}$ between $P^{(E)}$ and $P^{(\sigma)}$ in Fig. 1(c). Calculations are done with $R_aK_{\max}$ of 7, 8, 9, and 10. In this case $R_a = 2.5$ bohrs is chosen as the atomic sphere radius of the Al atom. In the following calculations, $1s$ and $2s$ states of Al are treated as core states and all other states up to $l_{\max} = 10$ are treated as valence states. All valence states except the $2p$ states are described using pure LAPW basis functions Eq. (1), while $2p$ states are represented using semicore local orbitals (LOs)—the second term in Eq. (2). We choose most of the input parameters higher than necessary for a regular total energy calculations in order to exclude possible numerical errors due to these parameters. The $G_{\max}$ in the expansion of the charge density [see Eq. (3)] and the potential in the interstitial is 20 $\text{Ry}^{\frac{1}{2}}$, and a k mesh is $(24 \times 24 \times 24)$. The standard tetrahedron method with Blöchl's correction [29] [Figs. 1(a)–1(c)], as well as the FD method with a broadening parameter of 0.005 Ry [Fig. 1(d)], for the integration in the irreducible Brillouin zone (IBZ) are used. All integrations in the interstitial region are evaluated using the fast Fourier transform (FFT) method with a FFT grid of $90 \times 90 \times 90$.

The total energy curves [Fig. 1(a)] show that the equilibrium volume and $P^{(E)}$ are insensitive to $R_aK_{\max}$ although

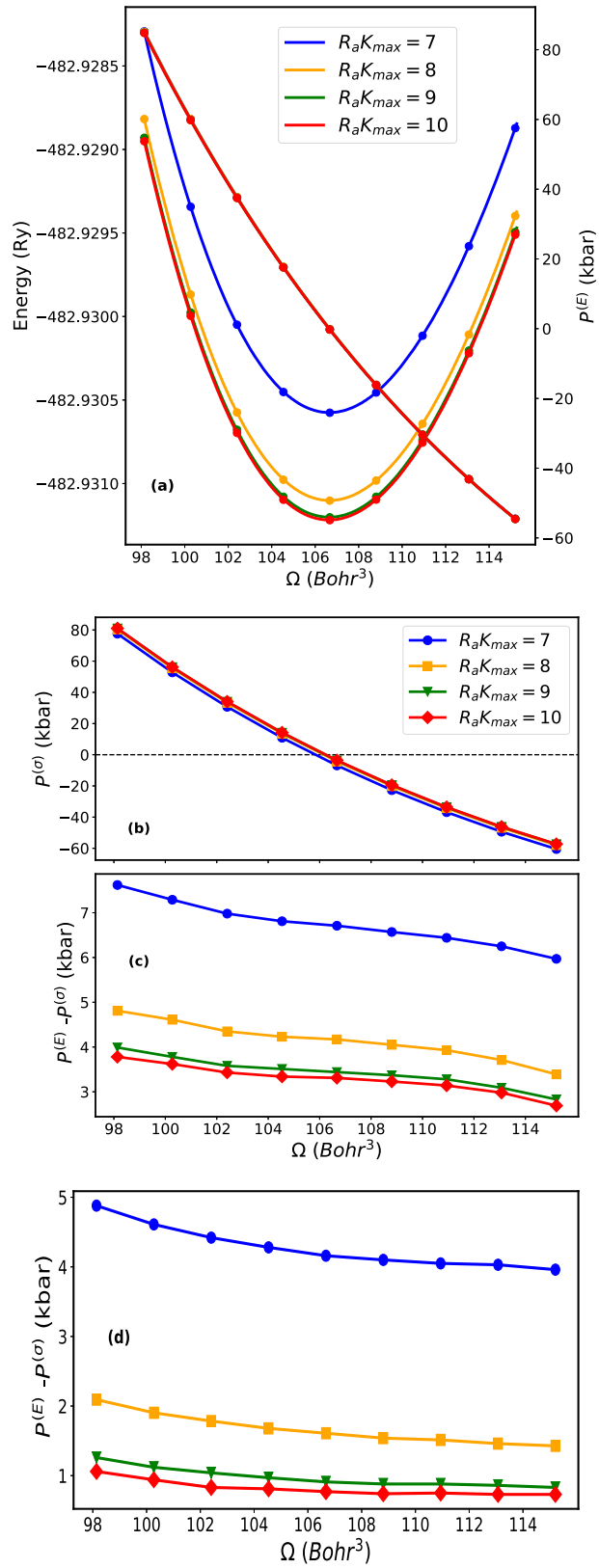

FIG. 1. (a) Energy-volume curves as well as $P^{(E)}$, (b) the negative trace of the full stress tensor $P^{(\sigma)}$, and (c) the difference between $P^{(\sigma)}$ and $P^{(E)}$ as a function of Ω for various $R_aK_{\max}$ for fcc Al. The standard tetrahedron method with the Blöchl correction is used in (a)–(c), while the FD method with a 0.005 Ry broadening parameter is used for (d).

TABLE I. Predicted lattice constant a_0 (in bohrs) and bulk modulus B (in kbars) from the analytical stress tensor [superscript (σ)] and directly from the total energy [superscript (E)] as a function of $R_aK_{\max}$ for fcc Al. The standard tetrahedron method with Blöchl's correction is used for k-space integration.

$R_aK_{\max}$	$a_0^{(\sigma)}$	$a_0^{(E)}$	$B^{(\sigma)}$	$B^{(E)}$
7	7.508	7.528	871	844
8	7.516	7.528	859	844
9	7.518	7.528	857	843
10	7.518	7.528	856	843

TABLE II. Predicted lattice constant a_0 (in bohrs) and bulk modulus B (in kbars) from the analytical stress tensor formalism [superscript (σ)] and directly from the total energy [superscript (E)] as a function of $R_aK_{\max}$ for fcc Al. The FD method with a broadening parameter of 0.005 Ry is used.

$R_aK_{\max}$	$a_0^{(\sigma)}$	$a_0^{(E)}$	$B^{(\sigma)}$	$B^{(E)}$
7	7.513	7.526	854	838
8	7.521	7.526	843	839
9	7.523	7.526	841	838
10	7.523	7.526	840	837

the magnitude of the total energy does change with $R_aK_{\max}$. As a result, $P^{(E)}$ barely changes, which can also be seen in the resulting prediction for the equilibrium lattice parameter shown in Table I. The pressure $P^{(\sigma)}$ estimated from the stress tensor shown in Fig. 1(b) clearly shows a $R_aK_{\max}$ dependency. However, this dependency, which can also be seen in Fig. 1(c), only manifests itself at the third decimal place in the predicted lattice parameter provided $R_aK_{\max}$ is chosen greater than 7 (see Table I). All calculations in Figs. 1(a)–1(c) were done with the Blöchl correction [29] in the tetrahedron method. We also repeated the same calculation without Blöchl's correction and found that this correction neither improved nor worsened the results. Aluminum is a metallic system with a complicated Fermi surface and has partial occupations close to the Fermi level. When deriving stress tensor formulas, we assumed that the occupancy does not depend on the strain in a first-order approximation. The underlying reasoning for this assumption, which is also supported for the closely related force calculations [3], is that the number of electrons in the system is conserved and thus the change in the occupation numbers is a second-order effect. For the system with partial occupations, however, Ref. [30] reports that when calculating forces, the total energy given in Eq. (4) is not variational and needs to be replaced by the more general expression

$$F = E_{\text{tot}} - \sum_{vk} n_{vk}\sigma S, \tag{24}$$

in which F denotes the Helmholtz free energy, S is the entropy, and $\sigma = k_BT$, where T and k_B denote the temperature and Boltzmann's constant, respectively. Similar to what is observed in the force formalism, we expect that when calculating the strain variation of the second term of Eq. (24), a corresponding term will be canceled when the strain variation of the occupation number is computed. In Ref. [30] an explicit equation for S is given for the Fermi-Dirac distribution function. We repeated the above calculations [Figs. 1(a)–1(c)] using the FD method which is shown in Fig. 1(d). The comparison of Figs. 1(c) and 1(d), and Tables I and II shows that the analytical stress tensor and thereby the predicted lattice constant $a_0^{(\sigma)}$ from the stress tensor improves significantly. These tables also show that there is a small change in the total energy, affecting $a_0^{(E)}$ only in the third digit, but more noticeable in the bulk modulus. The effect on the analytical stress calculation, on the other hand, is much stronger, as can be seen from comparing the $a_0^{(\sigma)}$ columns of Tables I and II. Moreover, unless we choose $R_aK_{\max}$ as small as 7, the discrepancy between $P^{(E)}$ and $P^{(\sigma)}$ manifests itself only in the third digit place of the predicted lattice constants $a_0^{(\sigma)}$ when the FD method is used, which certainly appears to be acceptable in standard electronic structure calculations. Tables I and II show that $R_aK_{\max} = 8$ is sufficient for the FD method, while at $R_aK_{\max} = 10$ a difference of 0.01 bohrs between $a_0^{(E)}$ and $a_0^{(\sigma)}$ persist using the tetrahedron method. Figures 1(c) and 1(d) also reveal a stronger volume dependency of $P^{(E)} - P^{(\sigma)}$ calculated using the tetrahedron method as compared to the FD method.

The convergence of the stress tensor with respect to k mesh with the two different BZ sampling methods, the tetrahedron and FD method, is shown in Fig. 2. Two different k-mesh grids of $15 \times 15 \times 15$ and $24 \times 24 \times 24$ are used. The results show that $P^{(E)} - P^{(\sigma)}$ in the FD method is fairly insensitive to the choice of the k mesh while with the tetrahedron method there

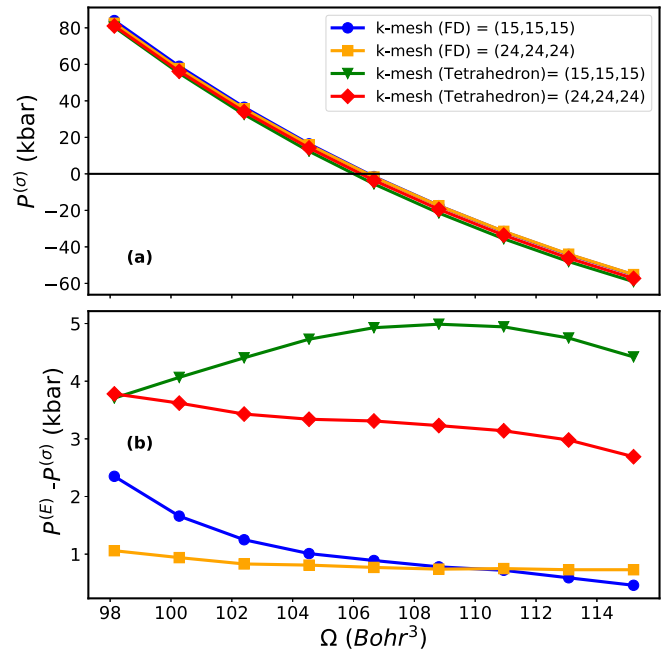

FIG. 2. (a) Analytical pressure $P^{(\sigma)}$ and (b) the difference between $P^{(\sigma)}$ and $P^{(E)}$ for two different k-mesh grids as function of Ω for fcc Al. The BZ is sampled using the FD method with smearing 0.005 Ry and the tetrahedron method with Blöchl's correction. $R_aK_{\max} = 10$ and all the remaining input parameters are the same as in Fig. 1.

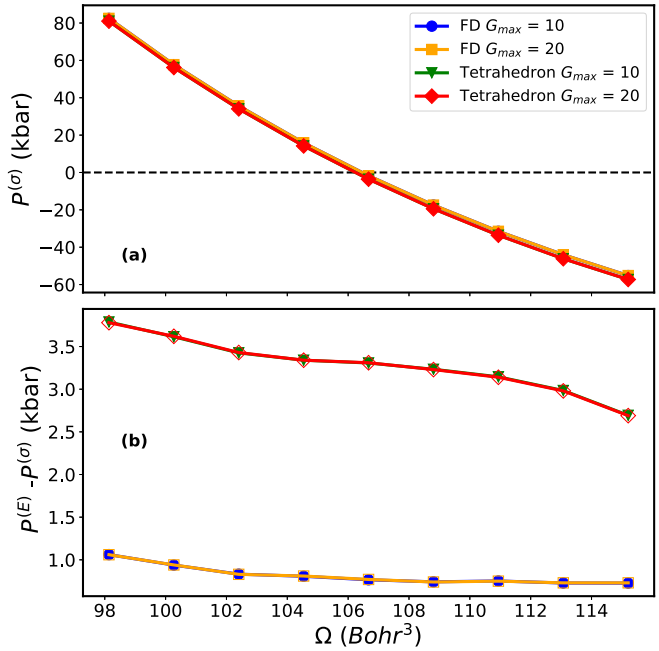

FIG. 3. (a) Analytical pressure $P^{(\sigma)}$ and (b) the difference between $P^{(\sigma)}$ and $P^{(E)}$ for the different $G_{\max}$ for the charge density and the potential as function of Ω for fcc Al. The FD method and tetrahedron method with Blöchl's correction are used for BZ sampling. $R_aK_{\max} = 10$ and all the remaining input parameters are the same as in Fig. 1.

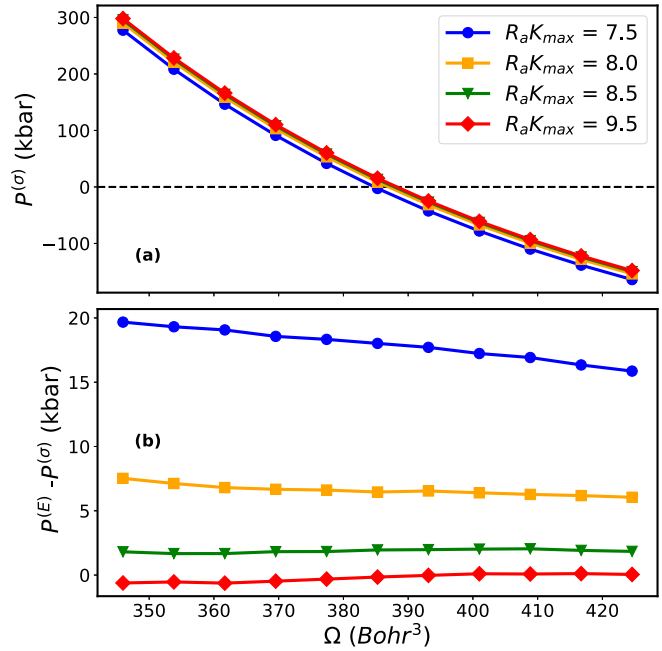

FIG. 4. (a) Analytical pressure $P^{(\sigma)}$ and (b) the difference between $P^{(\sigma)}$ and $P^{(E)}$ for the four different values of $R_aK_{\max}$ as a function of Ω for $SrTiO_3$.

is a change in the predicted lattice constant $a_0^{\sigma} = 7.512$ bohrs ($15 \times 15 \times 15$) to 7.518 bohrs ($24 \times 24 \times 24$).

The convergence of the stress tensor with respect to the value of the cutoff $G_{\max}$ of the expansion of the charge density and the potential in the interstitial is shown in Fig. 3. The figure shows that $P^{(\sigma)}$ is insensitive to the choice of $G_{\max}$. Thus, the same value of $G_{\max}$ can be used for the total energy and stress calculations.

B. $SrTiO_3$

Next, we considered $SrTiO_3$ in the cubic perovskite structure with space group $Pm\bar{3}m$. All states up to $3d$, $2p$, and $1s$ are considered as the core states for Sr, Ti, and O, respectively. All other states are treated as valence states and described with LAPW+LO basis functions. Calculations are carried out with $G_{\max} = 20$ $\mathrm{Ry}^{\frac{1}{2}}$, $L_{\max}^{\mathrm{ns}}$ equals 6, and the BZ is sampled on a tetrahedron mesh with ten intervals in each direction. The convergence of the stress tensor according to the different values of $R_aK_{\max}$ is presented in Fig. 4. Calculated pressure $P^{(\sigma)}$ from the negative trace of the stress tensor is shown in Fig. 4(a) and its difference with the pressure $P^{(E)}$ is shown in Fig. 4(b). The lattice parameters resulting from the stress tensor are 7.273, 7.286, 7.292, and 7.295 bohrs for $R_aK_{\max} = 7.5$, 8, 8.5, and 9, respectively. This value is fairly close to the 7.295 bohrs predicted from total energy, with the exception of $R_aK_{\max} = 7.5$. This indicates that $R_aK_{\max} = 8$ is sufficient to obtain the lattice parameter with a precision 0.01 bohrs.

Figure 5 shows the convergence of the stress tensor with respect to three different k meshes $8 \times 8 \times 8$, $10 \times 10 \times 10$, and $15 \times 15 \times 15$ with $R_aK_{\max} = 8.5$. Since $SrTiO_3$ is an insulator, a smaller k mesh should be sufficient in calculation, which can also be seen in Fig. 5. Figure 5(b) indicates that the difference $P^{(E)} - P^{(\sigma)}$ between the trace of the stress tensor and the energy-based pressure estimate $P^{(E)}$ remains the same

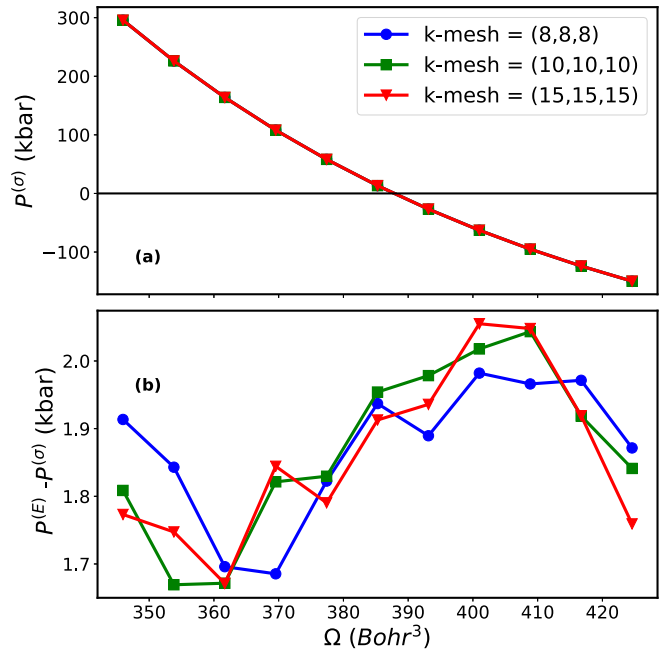

FIG. 5. (a) Analytical pressure $P^{(\sigma)}$ and (b) the difference between $P^{(\sigma)}$ and $P^{(E)}$ for the three different k meshes as a function of Ω for $SrTiO_3$. $R_aK_{\max} = 8.5$ and all the remaining input parameters are the same as in Fig. 4.

TABLE III. Comparison of the equilibrium lattice parameter a_0 (in bohrs) and the bulk modulus (in kbars) obtained from the total energy and directly from the stress tensor for different compounds.

Elements	$a_0^{(\sigma)}$	$a_0^{(E)}$	$B^{(\sigma)}$	$B^{(E)}$
NaCl	10.331	10.334	324	323
LaN	9.880	9.894	1209	1226
TiN	7.900	7.904	3182	3192
NbC	8.395	8.398	3254	3265
MgS	10.590	10.578	621	616
AlAs	10.654	10.659	768	763
$SrTiO_3$	7.295	7.295	2004	2007

for all selected k meshes. Table III compares the structural parameters of several cubic compounds obtained from $P^{(E)} = 0$ and $P^{(\sigma)} = 0$, and very good overall agreement has been found.

C. ZnO

Calculations for ZnO in the hexagonal wurtzite structure are carried out with sphere sizes of 1.95 and 1.68 bohrs for Zn and O, respectively. For Zn all states up to $3s$ and for O the $1s$ states are considered as core states. We choose a cutoff of $G_{\max} = 20$ $\mathrm{Ry}^{\frac{1}{2}}$ in the expansion of the charge density and the potential. The $R_a K_{\max}$ value is 9.5, the k-point grid is $12 \times 12 \times 6$, $L_{\max}^{\mathrm{ns}} = 6$, and the exchange-correlation energy and potential are calculated using the LDA. Our investigation starts with a total energy calculation for a unit cell based on the experimental lattice parameters. We performed a two-dimensional (2D) optimization of a and c, using either the calculated total energies or the stress tensor elements σ_{11} and σ_{33}. The first and second rows of Table IV offer a comparison of these values with their corresponding counterparts predicted from the stress tensor formalism.

In the total energy calculation, both the core charge density and the potential are considered to be spherically symmetric and only the $lm = 00$ term in a lattice harmonic expansion contributes. On the other hand, in our stress tensor formalism when calculating the core correction Eq. (21), the potential V_{eff} can have nonspherical components, which are described by higher angular momentum quantum numbers. However, in the final expression Eq. (E3), due to the presence of Gaunt number $G_{l,1,1}^{-m,t,t'}$ and Kronecker deltas $\delta_{1,l+s}\delta_{-t',m+t}$, only $lm = 00$ and $2m$ components of the potential are allowed to be nonzero, such that we are left with $V_{\mathrm{tot}}^c = V_{00}^c + V_{2m}^c$, in which the term

TABLE IV. Comparison of the equilibrium lattice parameters a_0 and c_0 of ZnO obtained from a fifth-order polynomial fit to the total energy and directly from the stress tensor with (V_{tot}^c) and without (V_{00}^c) inclusion of the nonspherical components ($l = 2$) in the potential when the core correction is calculated using Eq. (G6).

	a_0 (bohrs)	c_0 (bohrs)
Energy	6.056	9.763
Stress with V_{tot}^c	6.057	9.762
Stress with V_{00}^c	6.030	9.849

TABLE V. Comparison of σ_{33} (in kbars) calculated using Eqs. (25) and (18) for silicon in the diamond structure with seven different nonvolume conserving tetragonal deformations. The superscripts (E) and (σ) correspond to the energy and stress.

ϵ_{33}	$\sigma_{33}^{(E)}$	$\sigma_{33}^{(\sigma)}$
−0.020	33.12	34.28
−0.013	21.95	22.63
−0.007	10.90	11.17
0.000	0.00	0.00
0.007	−10.74	−10.99
0.013	−21.29	−21.70
0.020	−31.65	−32.16

with $lm = 00$ is the main contribution and the $lm = 2m$ component acts as an additional correction, which may or may not be zero. For instance, in highly (cubic) symmetric crystal structure there are no $lm = 2m$ terms in a lattice harmonic expansion, but in even in slightly lower symmetric crystal structures such as a hexagonal system, it was found that these contributions can become quite significant and neglecting this term would lead to substantial errors in the predicted lattice parameters a and c, as can be verified by comparing the second and third rows of Table IV.

In passing we note that similar observations can be made for the core correction of the force calculation, where the $l = 1$ contribution appears in the potential upon displacing the atoms. In contrary to our present approach, the authors in Ref. [17] assumed that the potential in the core correction is only spherically symmetric.

D. Accuracy of individual stress tensor components

So far we have validated the trace of the stress tensor as well as the individual diagonal compounds at zero strain in terms of the lattice parameters. To validate the accuracy of the individual components of the stress tensor at finite strain, our strategy is to extract them from total energy calculations of various strained systems and compare these values with those obtained from our analytical stress. In the following we take a cubic silicon structure at the equilibrium volume (pressure = 0 and $a_0 = 10.209$) and keep the lattice parameters a_0 and $b_0 = a_0 = 10.209$ fixed while varying the c lattice parameter. Using a family of such tetragonal but volume nonconserving deformations, the stress component σ_{33} [denoted as $\sigma_{33}^{(E)}$ in Table V] is calculated numerically by fitting total energies with a fourth-order polynomial as a function of strain $\epsilon_{33} = \frac{c}{c_0} - 1$, and $\epsilon_{33} = 0$ and c_0 correspond to the equilibrium state at hydrostatic pressure zero. Now it is easy to see that the identity

$$\sigma_{33} = \frac{1}{\Omega_0}\frac{\partial E(\epsilon_{33})}{\partial \epsilon_{33}} \tag{25}$$

holds. Therefore, differentiating the above fourth-order polynomial fit, we readily obtain the stress values $\sigma_{33}^{(E)}$ recorded in Table V. On the other hand, a stress component $\sigma_{33} \equiv \sigma_{33}^{(\sigma)}$ can be calculated directly from Eq. (18). The input settings for these calculation were $R_a K_{\max} = 9.0$, $G_{\max} = 20$ for the charge density and the potential, k mesh = $(12 \times 12 \times 12)$,

and c is calculated as $c = (1 + \epsilon_{33})c_0$. A comparison of $\sigma_{33}^{(E)}$ and $\sigma_{33}^{(\sigma)}$ in Table V suggests that the calculated stress is also satisfactory for nonhydrostatic conditions. The table shows a small discrepancy between $\sigma_{33}^{(\sigma)}$ and $\sigma_{33}^{(E)}$, but similar calculations for different materials show that these numerical differences are within acceptable limits.

IV. SURVEY OF PREVIOUS ATTEMPTS IN LITERATURE

In chronological order, previous works on the stress tensor in the LAPW method are (A) Thonhauser *et al.* [17] which summarizes his 2001 Ph.D. thesis [18], (B) the two papers by Nagasako and Oguchi [19,20], and most recently (C) the diploma thesis of Klüppelberg [21].

A. The implementation by Thonhauser *et al.*

A first attempt to implement the stress tensor in the LAPW method dates back to the work of Thonhauser *et al.* [18] and was implemented in the WIEN97 code [24]. However, in Ref. [17] only results for Al and Si subject to hydrostatic pressure were shown, whereas the functionality and usefulness of this formalism for low symmetric noncubic materials remained unclear. Unfortunately, in Ref. [17] the final equations that have been implemented are not explicitly stated. Therefore we can only conjecture that our present formalism probably differs from Thonhauser's by the treatment of the electrostatic part of the stress tensor. Moreover, Ref. [17] uses a spherically symmetric potential for the core correction, whereas in our derivation [Eq. (21)] the potential can have nonspherical components. In addition, in contrast to Ref. [18], our formalism does not include the so-called discontinuity correction. Furthermore, an integration in the valence correction [the first term of Eq. (12) in this paper], is calculated in Ref. [18] over the whole unit cell, but using Eq. (13) we only need to calculate this inside the atomic spheres.

B. The implementation by Nagasako and Oguchi

In their two papers published in 2011 and 2013, Nagasako and Oguchi present a stress tensor calculation based on a modified version of the LAPW method proposed by Soler and Williams [22,23]. In Refs. [19,20] they provide a rigorous mathematical formalism for both local and semilocal functionals [31,32], respectively, and test their implementation for many different elements with different cutoff parameters and also for some compounds. The results are in good agreement with numerical results calculated directly from total energies. Regrettably, their implementation cannot easily be transferred to the standard LAPW method, since Soler-Williams basis functions are constructed in a related but nevertheless distinctly different way. In the Soler and Williams LAPW method, the plane waves are augmented only for the chemically important l ($l \leqslant l_{\max} : l_{\max} = 2$ or 3) inside the spherical region and the charge density and potential are formulated differently, which leads to a number of differences in the final expressions.

C. The diploma thesis of Klüppelberg

In his 2012 diploma thesis [21], Klüppelberg gave a very elegant mathematical derivation of the stress tensor and also discussed an implementation into the FLEUR code [33], which is based on the standard LAPW method. In particular, we would like to mention that this work contains a number of quite ingenious mathematical tricks, and fully tries to lay out the electrostatic part of the stress tensor. Tragically, as is honestly and in great detail documented in Klüppelberg's thesis, even for the hydrostatic component of the stress tensor the numerical tests showed a large disagreement of the resulting implementation with results of the so-called simple pressure formula and both differ from the results obtained directly from total energy fits. Our first attempt was to work with the formalism of Ref. [21], but this resulted in a huge error whose origin still remains unclear as of today. Our formalism differs from that presented in Ref. [21] by the treatment of the electrostatic part of the stress tensor and the absence of a so-called discontinuity correction.

V. DISCUSSION

In this paper we presented the stress tensor formalism in the all-electron full potential LAPW plus local orbital (LO) method. With this formalism, the core calculation can be fully relativistic, but the valence calculation is limited to the nonrelativistic limit. Substantial convergence tests were carried out and the calculations for metals, semiconductors, low symmetric crystal structure, and many compounds were presented. The accuracy of the stress tensor was validated by comparing the lattice parameters predicted from the stress tensor formalism and from total energy calculations. In addition, the accuracy of the individual components of the stress tensor was also tested in the nonhydrostatic case.

ACKNOWLEDGMENTS

K.B. and A.T. acknowledge support by the Austrian Science Fund (FWF) Project No. P27738-N28. K.B. would like to thank F. Tran for valuable discussions.

APPENDIX A: STRAIN DERIVATIVE OF VECTORS AND VOLUME

When strain is applied to a solid, a vector $\boldsymbol{V}$ changes as $\boldsymbol{V} \to \boldsymbol{V}[\underline{\underline{\epsilon}}] = (\underline{\underline{1}} \pm \underline{\underline{\epsilon}})\boldsymbol{V}$, the sign $\pm$ being positive for a the real space vector and negative for a reciprocal one. The unit cell volume changes as $\Omega \to \Omega[\underline{\underline{\epsilon}}] = \det(\underline{\underline{1}} + \underline{\underline{\epsilon}})\Omega$. When calculating the stress, the strain derivative of these quantities at vanishing strain is calculated as

$$\left.\frac{d\boldsymbol{V}[\underline{\underline{\epsilon}}]}{d\epsilon_{\alpha\beta}}\right|_{\underline{\underline{\epsilon}}=0} = \pm\frac{V}{2}(\widehat{\boldsymbol{V}}_\alpha\widehat{\boldsymbol{e}}_\beta + \widehat{\boldsymbol{V}}_\beta\widehat{\boldsymbol{e}}_\alpha) = \pm\frac{\boldsymbol{V}_\alpha\boldsymbol{V}_\beta}{V}, \quad \text{(A1)}$$

$$\left.\frac{d\Omega[\underline{\underline{\epsilon}}]}{d\epsilon_{\alpha\beta}}\right|_{\underline{\underline{\epsilon}}=0} = \delta_{\alpha\beta}\Omega, \quad \text{(A2)}$$

where $\frac{d}{d\epsilon_{\alpha\beta}}\det(\underline{\underline{1}} + \underline{\underline{\epsilon}})|_{\underline{\underline{\epsilon}}=0} = \delta_{\alpha\beta}$, $V = |\boldsymbol{V}|$, and $\boldsymbol{V}_\alpha$ is the Cartesian component of vector $\boldsymbol{V}$ in the direction $\alpha = 1, 2, 3$.

APPENDIX B: STRAIN DERIVATIVE OF INTEGRALS OVER THE UNIT CELL VOLUME

The total energy given in Eq. (4) contains the integration of the charge density times the potential over the unit cell volume. To perform the stress tensor calculation, this definition must be carried over to the strained system, differentiated with respect to the strain, and subsequently evaluated at zero strain. From such a derivative we obtain two contributions: (i) one that results from the variation of the unit cell volume and (ii) another one that results from the actual strain variation of the integrand. To clarify the discussion, consider a generic integral $\int_\Omega d^3\boldsymbol{r}F(\boldsymbol{r})$ of an arbitrary function $F(\boldsymbol{r})$ over the unit cell. The generic function $F(\boldsymbol{r})$, in practice, may refer to the charge density times a potential or some other physical quantity. Under application of strain it changes to $\int_{\Omega[\underline{\underline{\epsilon}}]} d^3\boldsymbol{r}_\epsilon F[\underline{\underline{\epsilon}}](\boldsymbol{r}_\epsilon)$. Differentiation of this integral with respect to a strain component $\epsilon_{\alpha\beta}$ gives

$$\left.\frac{d}{d\epsilon_{\alpha\beta}}\right|_{\underline{\underline{\epsilon}}=0}\int_{\Omega[\underline{\underline{\epsilon}}]} d^3\boldsymbol{r}_\epsilon F[\underline{\underline{\epsilon}}](\boldsymbol{r}_\epsilon)=\left.\frac{d}{d\epsilon_{\alpha\beta}}\right|_{\underline{\underline{\epsilon}}=0}\det(\underline{\underline{1}}+\underline{\underline{\epsilon}})\int_\Omega d^3\boldsymbol{r}F[\underline{\underline{\epsilon}}](\boldsymbol{r}[\underline{\underline{\epsilon}}])=\delta_{\alpha\beta}\int_\Omega d^3\boldsymbol{r}F(\boldsymbol{r})+\int_\Omega d^3\boldsymbol{r}\left.\frac{dF[\underline{\underline{\epsilon}}](\boldsymbol{r}[\underline{\underline{\epsilon}}])}{d\epsilon_{\alpha\beta}}\right|_{\underline{\underline{\epsilon}}=0}. \tag{B1}$$

In general, $\frac{dF[\underline{\underline{\epsilon}}](\boldsymbol{r}[\underline{\underline{\epsilon}}])}{d\epsilon_{\alpha\beta}}|_{\underline{\underline{\epsilon}}=0}$ may depend on $\underline{\underline{\epsilon}}$ both explicitly via linear response and implicitly via its smeared argument $\boldsymbol{r}[\underline{\underline{\epsilon}}]$, which implies that

$$\left.\frac{dF[\underline{\underline{\epsilon}}](\boldsymbol{r}[\underline{\underline{\epsilon}}])}{d\epsilon_{\alpha\beta}}\right|_{\underline{\underline{\epsilon}}=0}=\left.\frac{dF[\underline{\underline{\epsilon}}](\boldsymbol{r})}{d\epsilon_{\alpha\beta}}\right|_{\underline{\underline{\epsilon}}=0}+\left.\frac{d\boldsymbol{r}[\underline{\underline{\epsilon}}]}{d\epsilon_{\alpha\beta}}\right|_{\underline{\underline{\epsilon}}=0}\cdot\boldsymbol{\nabla}F(\boldsymbol{r}), \tag{B2}$$

where $\frac{d\boldsymbol{r}[\underline{\underline{\epsilon}}]}{d\epsilon_{\alpha\beta}}=\frac{r}{2}(\widehat{\boldsymbol{r}}_\alpha\widehat{\boldsymbol{e}}_\beta+\widehat{\boldsymbol{r}}_\beta\widehat{\boldsymbol{e}}_\alpha)=r\widehat{\boldsymbol{r}}_\alpha\widehat{\boldsymbol{r}}_\beta$. If we substitute Eq. (B2) into (B1), we arrive at

$$\left.\frac{d}{d\epsilon_{\alpha\beta}}\right|_{\underline{\underline{\epsilon}}=0}\int_{\Omega[\underline{\underline{\epsilon}}]} d^3\boldsymbol{r}_\epsilon F[\underline{\underline{\epsilon}}](\boldsymbol{r}_\epsilon)=\delta_{\alpha\beta}\int_\Omega d^3\boldsymbol{r}F(\boldsymbol{r})+\int_\Omega d^3\boldsymbol{r}\left.\frac{dF[\underline{\underline{\epsilon}}](\boldsymbol{r})}{d\epsilon_{\alpha\beta}}\right|_{\underline{\underline{\epsilon}}=0}+\frac{1}{2}\int_\Omega d^3\boldsymbol{r}(r_\beta\partial_\alpha+r_\alpha\partial_\beta)F(\boldsymbol{r}). \tag{B3}$$

APPENDIX C: PARTIAL DERIVATIVE OF THE WAVE FUNCTION

Spatial partial derivatives of the wave function $\psi^{\mathrm{v}}_{v\boldsymbol{k}}(\boldsymbol{r})$ in the LAPW basis representation [Eq. (2)] are required to compute the second line of Eq. (14).

(1) In the interstitial region, the LAPW basis functions Eq. (1) are plane waves, and thus

$$\begin{aligned}\partial_\alpha\psi^{\mathrm{v\,IS}}_{v\boldsymbol{k}}(\boldsymbol{r})&=\sum_{\boldsymbol{K}}c_{v\boldsymbol{k}\boldsymbol{K}}\,\partial_\alpha\frac{1}{\sqrt{\Omega}}e^{i(\boldsymbol{k}+\boldsymbol{K})\cdot\boldsymbol{r}}\\&=\sum_{\boldsymbol{K}}c_{v\boldsymbol{k}\boldsymbol{K}}\,i(\boldsymbol{k}+\boldsymbol{K})_\alpha\frac{1}{\sqrt{\Omega}}e^{i(\boldsymbol{k}+\boldsymbol{K})\cdot\boldsymbol{r}}.\end{aligned} \tag{C1}$$

(2) To compute the gradient components $\partial_\alpha\psi^{\mathrm{v}\,R_a}_{v\boldsymbol{k}}(\boldsymbol{r})$ in the atomic spheres, where the valence wave function is represented by the spherical harmonics expansion [Eq. (1)], we need the derivatives

$$\partial_\alpha Y_{lm}(\hat{\boldsymbol{r}}_a)=\frac{1}{r}\sum_{s=\pm1}\sum_{t=-1}^{1}c^{st}_\alpha(l,m)Y_{l+s,m+t}(\hat{\boldsymbol{r}}_a), \tag{C2}$$

$$\partial_\alpha u_{l\lambda}(r_a)=\widehat{r}_{a\alpha}u'_{l\lambda}(r_a), \tag{C3}$$

where $c^{st}_\alpha(l,m)$ is calculated as follows,

$$c^{st}_\alpha(l,m)=\oint_S dsr\partial_\alpha Y_{lm}(\hat{r})Y^*_{l+s,m+t}(\hat{r}), \tag{C4}$$

Abbreviating $u_{l\lambda}(r_a,E^a_{l\lambda})$ and $Y_{lm}(\hat{\boldsymbol{r}}_a)$ by the shorthand notations $u_{l\lambda}(r_a)$ and Y_{lm}, respectively, we have

$$\begin{aligned}\partial_\alpha(u_{l\lambda}(r_a)Y_{lm})&=\hat{r}_{a\alpha}u'_{l\lambda}(r_a)Y_{lm}\\&\quad+\frac{u_{l\lambda}(r_a)}{r}\sum_{s=\pm1}\sum_{t=-1}^{1}c^{st}_\alpha(l,m)Y_{l+s,m+t}.\end{aligned} \tag{C5}$$

The unit vector component $\widehat{\boldsymbol{r}}_{a\alpha}$ along the Cartesian direction α can be expanded as

$$\widehat{\boldsymbol{r}}_{a\alpha}=\sum_{t=-1}^{1}c_{\alpha t}Y_{1t}(\hat{\boldsymbol{r}}), \tag{C6}$$

where $c_{\alpha t}$ can be obtained using the orthogonality property of spherical harmonics as follows,

$$c_{\alpha t}=\oint_S ds\hat{\boldsymbol{r}}_\alpha Y^*_{1t}(\hat{\boldsymbol{r}}), \tag{C7}$$

and the product of two spherical harmonics is expanded into Gaunt numbers times another spherical harmonics, i.e.,

$$Y_{1t}Y_{lm}=\sum_{s,v}G^{v,t,m}_{s,1,l}Y_{s,v}. \tag{C8}$$

In summary, the partial derivative of the wave function inside the atomic sphere is

$$\begin{aligned}\partial_\alpha\psi^{\mathrm{v}\,R_a}_{v\boldsymbol{k}}(\boldsymbol{r})=\sum_{\boldsymbol{K}}c_{v\boldsymbol{k}\boldsymbol{K}}\Bigg[&\sum_{t=-1}^{1}c_{\alpha t}u'_{l\lambda}(r)\sum_{s,v}G^{v,t,m}_{s,1,l}Y_{sv}(\hat{\boldsymbol{r}}_a)\\&+\frac{u_{l\lambda}(r)}{r}\sum_{s=\pm1}\sum_{t=-1}^{1}c^{st}_\alpha(l,m)Y_{l+s,m+t}(\hat{\boldsymbol{r}}_a)\Bigg].\end{aligned} \tag{C9}$$

The mathematical steps provided in this Appendix are used to simplify the valence kinetic stress tensor $\sigma^{\mathrm{val,kin}}_{\alpha\alpha}$ of Eq. (18).

APPENDIX D: STRAIN VARIATION OF THE BASIS FUNCTION

The strain variation of the basis function is required to calculate the valence correction stress $\sigma^{\mathrm{val,corr}}_{\alpha\beta}$ of Eq. (18). In

the discussion following Eq. (13), we have argued that calculating the valence correction requires only to calculate the strain variation of $\phi_{\boldsymbol{k}[\underline{\underline{\epsilon}}]\boldsymbol{K}[\underline{\underline{\epsilon}}]}[\underline{\underline{\epsilon}}](\boldsymbol{r}[\underline{\underline{\epsilon}}])\sqrt{\Omega[\underline{\underline{\epsilon}}]}$ inside the atomic spheres. Indeed, expanding the strained version of the LAPW basis functions restricted to the interstitial region, we see that

$$\sqrt{\Omega[\underline{\underline{\epsilon}}]}\phi^{\mathrm{IS}}_{\boldsymbol{k}[\underline{\underline{\epsilon}}]\boldsymbol{K}[\underline{\underline{\epsilon}}]}[\underline{\underline{\epsilon}}](\boldsymbol{r}[\underline{\underline{\epsilon}}]) = e^{i(\boldsymbol{k}+\boldsymbol{K})[\underline{\underline{\epsilon}}]\cdot\boldsymbol{r}[\underline{\underline{\epsilon}}]} = \sqrt{\Omega}\phi^{\mathrm{IS}}_{\boldsymbol{k}\boldsymbol{K}}(\boldsymbol{r}) + O(\underline{\underline{\epsilon}}^2), \quad \text{(D1)}$$

as claimed. Thus, in the interstitial region $\frac{d}{d\epsilon_{\alpha\beta}}\phi^{\mathrm{IS}}_{\boldsymbol{k}[\underline{\underline{\epsilon}}]\boldsymbol{K}[\underline{\underline{\epsilon}}]}[\underline{\underline{\epsilon}}](\boldsymbol{r}[\underline{\underline{\epsilon}}])\sqrt{\Omega[\underline{\underline{\epsilon}}]} = O(\underline{\underline{\epsilon}})$ and does not contribute to the valence correction stress. It remains to calculate the first-order strain variation of $\sqrt{\Omega[\underline{\underline{\epsilon}}]}\phi_{\boldsymbol{k}[\underline{\underline{\epsilon}}]\boldsymbol{K}[\underline{\underline{\epsilon}}]}[\underline{\underline{\epsilon}}](\boldsymbol{r}[\underline{\underline{\epsilon}}])$ in the atomic spheres. In the deformed system, a basis function inside the atomic sphere region as defined in Eq. (1) becomes

$$\phi_{\boldsymbol{k}[\underline{\underline{\epsilon}}]\boldsymbol{K}[\underline{\underline{\epsilon}}]}[\underline{\underline{\epsilon}}](\boldsymbol{r}[\underline{\underline{\epsilon}}]) = \sum_{lm\lambda} a^{a\boldsymbol{k}[\underline{\underline{\epsilon}}]\boldsymbol{K}[\underline{\underline{\epsilon}}]}_{lm\lambda} u_{l\lambda}[\underline{\underline{\epsilon}}](r_a[\underline{\underline{\epsilon}}])Y_{lm}(\hat{\boldsymbol{r}}_a[\underline{\underline{\epsilon}}]). \quad \text{(D2)}$$

Here, the index λ (= 0, 1) is introduced to provide a compact notation including both the radial part and the energy derivative part of the basis function Eq. (1). All terms with $[\underline{\underline{\epsilon}}]$ are meant to be defined in the strained system. Furthermore,

$$\frac{d}{d\epsilon_{\alpha\beta}}\left[\sqrt{\Omega[\underline{\underline{\epsilon}}]}\phi_{\boldsymbol{k}[\underline{\underline{\epsilon}}]\boldsymbol{K}[\underline{\underline{\epsilon}}]}[\underline{\underline{\epsilon}}](\boldsymbol{r}[\underline{\underline{\epsilon}}])\right]_{\underline{\underline{\epsilon}}=0} = \sum_{lm\lambda}\left[\frac{d}{d\epsilon_{\alpha\beta}}\sqrt{\Omega[\underline{\underline{\epsilon}}]}a^{a\boldsymbol{k}[\underline{\underline{\epsilon}}]\boldsymbol{K}[\underline{\underline{\epsilon}}]}_{lm\lambda}\right]_{\underline{\underline{\epsilon}}=0} u^a_{l\lambda}(r_a)Y_{lm}(\hat{\boldsymbol{r}}_a)$$
$$+\sqrt{\Omega}\sum_{lm\lambda} a^{a\boldsymbol{k}\boldsymbol{K}}_{lm\lambda}\left[\frac{d}{d\epsilon_{\alpha\beta}}u^a_{l\lambda}(r_a[\underline{\underline{\epsilon}}])\right]_{\underline{\underline{\epsilon}}=0} Y_{lm}(\hat{\boldsymbol{r}}_a) + \sqrt{\Omega}\sum_{lm\lambda} a^{a\boldsymbol{k}\boldsymbol{K}}_{lm\lambda}\, u^a_{l\lambda}(r_a)\left[\frac{d}{d\epsilon_{\alpha\beta}}Y_{lm}(\hat{\boldsymbol{r}}_a[\underline{\underline{\epsilon}}])\right]_{\underline{\underline{\epsilon}}=0}. \quad \text{(D3)}$$

In order to simplify this expression further, we repeatedly make use of the following relations:

(1) For the strain variation of spherical harmonics we use the general formula

$$\frac{dY_{lm}(\widehat{\boldsymbol{V}}[\underline{\underline{\epsilon}}])}{d\epsilon_{\alpha\beta}} = \pm\frac{1}{2}\sum_{s=\pm}\sum_{t=-1}^{1}\left[c^{st}_{\beta}(l,m)\widehat{\boldsymbol{V}}_{\alpha} + c^{st}_{\alpha}(l,m)\widehat{\boldsymbol{V}}_{\beta}\right]Y_{l+s,m+t}(\widehat{\boldsymbol{V}}), \quad \text{(D4)}$$

where the positive and negative sign applies to a real space vector and reciprocal space vector, respectively.

(2) Similarly, the strain variation of the spherical Bessel function, which is necessary to calculate the strain variation of the matching coefficient $a^{a\boldsymbol{k}[\underline{\underline{\epsilon}}]\boldsymbol{K}[\underline{\underline{\epsilon}}]}_{lm\lambda}$, is

$$\frac{d\, j_l(|\boldsymbol{V}[\underline{\underline{\epsilon}}]|R_a)}{d\epsilon_{\alpha\beta}} = \pm j_l'(|\boldsymbol{V}|R_a)V\widehat{\boldsymbol{V}}_{\alpha}\widehat{\boldsymbol{V}}_{\beta}. \quad \text{(D5)}$$

In addition, we resort to the frozen augmentation approximation, according to which the explicit strain dependency in $u^a_{l\lambda}[\underline{\underline{\epsilon}}](r_a[\underline{\underline{\epsilon}}])$ via the linear response is discarded while keeping only an implicit dependency via $r_a[\underline{\underline{\epsilon}}]$. Effectively, $u_{l\lambda}[\underline{\underline{\epsilon}}](r_a[\underline{\underline{\epsilon}}])$ is therefore replaced by $u_{l\lambda}(r_a[\underline{\underline{\epsilon}}])$:

$$\frac{du_{l\lambda}(r_a[\underline{\underline{\epsilon}}])}{d\epsilon_{\alpha\beta}} = u'_{l\lambda}(r_a)r_a\hat{r}_{a\alpha}\hat{r}_{a\beta}. \quad \text{(D6)}$$

Armed with these relations, we may tackle the numerical evaluation of the different terms that contribute in Eq. (D3). The necessary quantities to evaluate the strain variation of the basis function such as the variation of the reciprocal lattice vector, the unit cell volume, the spherical harmonics, and the spherical Bessel function are already given explicitly.

APPENDIX E: CORE CORRECTION STRESS TENSOR

The contribution of the core correction to the stress tensor as given in Eq. (21) is

$$\sigma^{\mathrm{core,corr}}_{\alpha\beta} = -\frac{1}{2\Omega}\sum_{a\in\Omega}\int_{R_a} d^3r\,\rho^a_c(\boldsymbol{r})(r_\beta\partial_\alpha + r_\alpha\partial_\beta)V_{\mathrm{eff}}(\boldsymbol{r}). \quad \text{(E1)}$$

To simplify the notation we replace $V_{\mathrm{eff}}(\boldsymbol{r})$ by $V(\boldsymbol{r})$, the potential expand in terms of spherical harmonics, ∂_α replace by $\hat{\boldsymbol{r}}_\alpha\frac{\partial}{\partial r}$, expand the unit vector $\hat{\boldsymbol{r}}_\alpha$ as given in Eq. (C6), and the angular derivative of the spherical harmonics is computed as in Eq. (C5). Thus

$$r_\beta\partial_\alpha V(\boldsymbol{r}) = \sum_{l,m}\left(rV'_{l,m}(r)\sum_{t,t'=-1}^{1} c_{\alpha t}c_{\beta t'}Y_{1t'}(\hat{\boldsymbol{r}})Y_{1t}(\hat{\boldsymbol{r}})Y_{l,m}(\hat{\boldsymbol{r}}) + V_{l,m}(r)\sum_{s=\pm1}\sum_{t,t'=-1}^{1} c^{\mathrm{st}}_{\alpha}(l,m)c_{\beta t'}Y_{1t'}(\hat{\boldsymbol{r}})Y_{l+s,m+t}(\hat{\boldsymbol{r}})\right). \quad \text{(E2)}$$

The prime in $V'_{l,m}(r)$ denotes the radial derivative and the loop over l and s has to be such that $l+s$ is always positive. To get the final expression of the core correction $\sigma^{\mathrm{core,corr}}_{\alpha\beta}$, we replace the product of two spherical harmonics in Eq. (E2) by a Gaunt number times spherical harmonic according to Eq. (C8), interchange α and β in the expression of $r_\beta\partial_\alpha V(\boldsymbol{r})$, substituting

Eq. (E2) in Eq. (E1), and use $\rho_c^a(\boldsymbol{r}) = \rho_{00}^a(r_a)Y_{00}(\hat{r})$,

$$\begin{aligned}\Omega\sigma_{\alpha\beta}^{\text{core,corr}} &= \sum_{l,m}\sum_{t,t'=-1}^{1}\left(I_1 c_{\alpha t}c_{\beta t'}\frac{(-1)^m}{4\pi}G_{l,1,1}^{-m,t,t'}\right.\\ &\left.+ I_2\sum_{s=\pm1}\frac{c_\beta^{st}(l,m)c_{\alpha t'}+c_\alpha^{st}(l,m)c_{\beta t'}}{2}\frac{(-1)^{t'}}{4\pi}\delta_{1,l+s}\delta_{-t',m+t}\right),\end{aligned} \tag{E3}$$

with

$$I_1 = -\int_0^{R_a} r_a^3 dr_a\sqrt{4\pi}\rho_{00}^*(r_a)\frac{dV_{lm}(r_a)}{dr_a}, \tag{E4}$$

$$I_2 = -\int_0^{R_a} dr_a\sqrt{4\pi}r_a^2\rho_{00}^*(r_a)V_{lm}(r_a). \tag{E5}$$

Recall that for a Gaunt number $G_{l,1,1}^{-m,t,t'}$ to be nonzero, the indices $[l, 1, 1]$ are required to satisfy the triangle rule, their sum needs to be even, and $m + t + t'$ must be zero [34].

APPENDIX F: VARIATION OF THE COULOMB POTENTIAL

The Coulomb potential is evaluated using Weinert's method [27]. According to this method the interstitial potential is obtained using the real interstitial charge density and a pseudocharge density, which reproduces the current multipole moments inside the spheres and is zero in the interstitial. The interstitial potential as given in Ref. [27] is

$$V_C^I(\boldsymbol{r}) = \sum_{\boldsymbol{K}\neq0}\frac{4\pi}{\boldsymbol{K}^2}[\tilde{\rho}_a(\boldsymbol{K}) + \rho_I(\boldsymbol{K})]e^{i\boldsymbol{K}\cdot\boldsymbol{r}}, \tag{F1}$$

where $\rho_I(\boldsymbol{K})$ and $\tilde{\rho}_a(\boldsymbol{K})$ are the Fourier components of the interstitial charge density and the smooth pseudocharge density, respectively. In the strained environment,

$$\rho_I[\underline{\underline{\epsilon}}](\boldsymbol{K}[\underline{\underline{\epsilon}}]) = \frac{1}{\Omega[\underline{\underline{\epsilon}}]}\int_{\Omega[\underline{\underline{\epsilon}}]} d^3\boldsymbol{r}_\epsilon\rho_I[\underline{\underline{\epsilon}}](\boldsymbol{r}_\epsilon)e^{-i\boldsymbol{K}[\underline{\underline{\epsilon}}]\cdot\boldsymbol{r}_\epsilon}. \tag{F2}$$

The physically strained electronic charge density $\rho_I[\underline{\underline{\epsilon}}](\boldsymbol{r}_\epsilon)$ is replaced by the "smeared" charge density $\rho_I((\underline{\underline{1}}-\underline{\underline{\epsilon}})\boldsymbol{r}[\underline{\underline{\epsilon}}])$,

$$\begin{aligned}\rho_I[\underline{\underline{\epsilon}}](\boldsymbol{K}[\underline{\underline{\epsilon}}]) &= \frac{1}{\Omega[\underline{\underline{\epsilon}}]}\int_{\Omega[\underline{\underline{\epsilon}}]} d^3\boldsymbol{r}_\epsilon\rho_I((\underline{\underline{1}}-\underline{\underline{\epsilon}})\boldsymbol{r}[\underline{\underline{\epsilon}}])e^{-i\boldsymbol{K}[\underline{\underline{\epsilon}}]\cdot\boldsymbol{r}_\epsilon}\\ &= \frac{1}{\Omega}\int_\Omega d^3\boldsymbol{r}\rho_I((\underline{\underline{1}}-\underline{\underline{\epsilon}})(\underline{\underline{1}}+\underline{\underline{\epsilon}})\boldsymbol{r})e^{-i\boldsymbol{K}\cdot\boldsymbol{r}}\\ &= \rho_I(\boldsymbol{K}),\end{aligned} \tag{F3}$$

where $\boldsymbol{r}[\underline{\underline{\epsilon}}] = (\underline{\underline{1}}+\underline{\underline{\epsilon}})\boldsymbol{r}$, $\boldsymbol{K}[\underline{\underline{\epsilon}}] = (\underline{\underline{1}}-\underline{\underline{\epsilon}})\boldsymbol{K}$, and $\boldsymbol{K}[\underline{\underline{\epsilon}}]\cdot\boldsymbol{r}[\underline{\underline{\epsilon}}] = \boldsymbol{K}\cdot\boldsymbol{r}$. A concept similar to the one used for the plane wave charge density is used for the pseudocharge density $\tilde{\rho}_a$:

$$\tilde{\rho}_a[\underline{\underline{\epsilon}}](\boldsymbol{K}[\underline{\underline{\epsilon}}]) = \tilde{\rho}_a(\boldsymbol{K}). \tag{F4}$$

With the help of Eqs. (F3) and (F4), the interstitial Coulomb potential in the deformed system is written as

$$\begin{aligned}V_C[\underline{\underline{\epsilon}}](\boldsymbol{K}[\underline{\underline{\epsilon}}]) &= \frac{4\pi}{\boldsymbol{K}[\underline{\underline{\epsilon}}]^2}[\tilde{\rho}_a[\underline{\underline{\epsilon}}](\boldsymbol{K}[\underline{\underline{\epsilon}}]) + \rho_I[\underline{\underline{\epsilon}}](\boldsymbol{K}[\underline{\underline{\epsilon}}])]\\ &= \frac{4\pi}{\boldsymbol{K}[\underline{\underline{\epsilon}}]^2}[\tilde{\rho}_a(\boldsymbol{K}) + \rho_I(\boldsymbol{K})]\end{aligned} \tag{F5}$$

For our calculations, the strain derivative of Eq. (F5) is also required. Since the Fourier components of the plane wave charge density and the pseudocharge density are independent of strain, their derivatives do not contribute to the stress. Therefore,

$$\begin{aligned}\frac{d}{d\epsilon_{\alpha\beta}}V_C[\underline{\underline{\epsilon}}](\boldsymbol{K}[\underline{\underline{\epsilon}}])\Big|_{\underline{\underline{\epsilon}}=0} &= \frac{4\pi}{\boldsymbol{K}^2}2\hat{\boldsymbol{K}}_\alpha\hat{\boldsymbol{K}}_\beta[\tilde{\rho}_a(\boldsymbol{K}) + \rho_I(\boldsymbol{K})]\\ &= 2\hat{\boldsymbol{K}}_\alpha\hat{\boldsymbol{K}}_\beta V_C(\boldsymbol{K}),\end{aligned} \tag{F6}$$

where we made use of $\frac{d\boldsymbol{K}[\underline{\underline{\epsilon}}]}{d\epsilon_{\alpha\beta}} = -\frac{\hat{\boldsymbol{K}}_\alpha\hat{\boldsymbol{K}}_\beta}{K}$ and $\hat{\boldsymbol{K}}_\alpha = \frac{\boldsymbol{K}_\alpha}{K}$, and $V_C(\boldsymbol{K})$ is given in Eq. (F1). This formula is used to evaluate the Coulomb part of the electrostatic stress tensor in the interstitial region—the interstitial part of the second line of Eq. (16).

APPENDIX G: FINAL FORMULAS

In this Appendix we present the explicit expressions of Eqs. (19)–(23) that we implemented in the WIEN2K package:

$$\begin{aligned}\sigma_{\alpha\beta}^{\text{val,kin}} = \frac{1}{\Omega}\Bigg\{&-\sum_{\upsilon\boldsymbol{k}}n_{\upsilon\boldsymbol{k}}\sum_{\boldsymbol{K}\boldsymbol{K}'}c_{\upsilon\boldsymbol{k}\boldsymbol{K}}^*c_{\upsilon\boldsymbol{k}\boldsymbol{K}'}(\boldsymbol{k}+\boldsymbol{K}')_\alpha(\boldsymbol{k}+\boldsymbol{K}')_\beta\Theta(\boldsymbol{K}-\boldsymbol{K}') + \frac{1}{2}\sum_{\upsilon\boldsymbol{k}}n_{\upsilon\boldsymbol{k}}\sum_a\sum_{LL'}\sum_{\lambda\lambda'}A_{L'\lambda'}^{a\upsilon\boldsymbol{k}*}A_{L\lambda}^{a\upsilon\boldsymbol{k}}\\ &\times\Bigg\{\sum_{t,t'=-1}(c_{\alpha t}c_{\beta t'}+c_{\beta t}c_{\alpha t'})\sum_{s,\nu}G_{s,1,l}^{\nu,t,m}G_{l',1,s}^{m',t',\nu}\int_0^{R_a}r_a^2dr_a u_{l'\lambda'}(r)u''_{l\lambda}(r)\\ &+\sum_{t,t'=-1}\sum_{s,\nu}\sum_{s'=\pm1}G_{s,1,l}^{\nu,t,m}\left[c_{\alpha t}c_\beta^{s't'}(s,\nu)+c_{\beta t}c_\alpha^{s't'}(s,\nu)\right]\delta_{l',s+s'}\delta_{m',\nu+t'}\int_0^{R_a}r_a dr_a u_{l'\lambda'}(r)u'_{l\lambda}(r)\\ &+\sum_{s=\pm1}\sum_{t,t'=-1}^{1}\left[c_\alpha^{st}(l,m)c_{\beta t'}+c_\beta^{st}(l,m)c_{\alpha t'}\right]G_{l',1,l+s}^{m',t',m+t}\int_0^{R_a}r_a^2dr_a u_{l'\lambda'}(r)\left[\frac{u'_{l\lambda}(r)}{r}-\frac{u_{l\lambda}(r)}{r^2}\right]\\ &+\sum_{s,s'=\pm1}\sum_{t,t'=-1}^{1}\left[c_\alpha^{st}(l,m)c_\beta^{s't'}(l+s,m+t)+c_\beta^{st}(l,m)c_\alpha^{s't'}(l+s,m+t)\right]\delta_{l',l+s+s'}\delta_{m',m+t+t'}\int_0^{R_a}dr_a u_{l'\lambda'}(r)u_{l\lambda}(r)\Bigg\}\Bigg\},\end{aligned} \tag{G1}$$

where $A^{avk}_{L\lambda} = \sum_{\boldsymbol{K}} c_{v\boldsymbol{kK}} a^{a\boldsymbol{kK}}_{lm\lambda}$ and L is a shorthand for the double index (l, m);

$$\begin{aligned}
\sigma^{\mathrm{val,corr}}_{\alpha\beta} = \frac{2}{\Omega}\sum_{a}\sum_{v\boldsymbol{k}} n_{v\boldsymbol{k}}\,\mathrm{Re}\Bigg\{ & \sum_{L\lambda\lambda'} D^{av\boldsymbol{k}*}_{L\lambda}(\alpha,\beta) A^{av\boldsymbol{k}}_{L\lambda'}\Big[\big(E^a_l - \epsilon_{v\boldsymbol{k}}\big)\delta_{\lambda\lambda'}\big\|u^a_{l\lambda'}\big\|^2 + \delta_{\lambda'1}\delta_{\lambda,0}\Big] \\
& + \sum_{L\lambda}\sum_{L'\lambda'} A^{av\boldsymbol{k}*}_{L\lambda} A^{av\boldsymbol{k}}_{L'\lambda'} \sum_{t,,t'=-1} c_{\alpha t} c_{\beta t'} \sum_{s,v} G^{v,t,t'}_{s,1,1} G^{m,m',v}_{l,l',s}\Big[\big(E^a_{l'} - \epsilon^{\mathrm{v}}_{v\boldsymbol{k}}\big) J^{a\lambda\lambda'}_{ll'} + \delta_{\lambda'1} J^{a\lambda 0}_{ll'}\Big] \\
& + \frac{1}{2}\sum_{s=\pm1}\sum_{t,t'=-1}^{1}\big[c_{\alpha t'} c^{st}_{\beta}(l,m) + c_{\beta t'} c^{st}_{\alpha}(l,m)\big]\sum_{L'\lambda'} A^{av\boldsymbol{k}*}_{L\lambda} A^{av\boldsymbol{k}}_{L'\lambda'} G^{m,t',m+t}_{l,1,l+s}\Big\{\big(E^a_{l'} - \epsilon^{\mathrm{v}}_{v\boldsymbol{k}}\big)\delta_{\lambda,\lambda'}\big\|u^a_{l\lambda'}\big\|^2 + \delta_{\lambda'1}\delta_{\lambda,0}\Big\} \\
& + \sum_{L''>0}^{L^{\mathrm{ns}}_{\max}}\sum_{L\lambda}\sum_{L'\lambda'} D^{av\boldsymbol{k}*}_{L\lambda}(\alpha,\beta) A^{av\boldsymbol{k}}_{L'\lambda'} G^{m,m'',m'}_{l,l'',l'} V^{a\,\lambda\lambda'}_{l,L'',l'} \\
& + \sum_{L''>0}^{L^{\mathrm{ns}}_{\max}}\sum_{L\lambda}\sum_{L'\lambda'} A^{av\boldsymbol{k}*}_{L\lambda} A^{av\boldsymbol{k}}_{L'\lambda'} \sum_{t,,t'=-1}\sum_{sv}\sum_{s'v'} c_{\alpha t} c_{\beta t'} G^{v,t,t'}_{s,1,1} G^{v',m'',m'}_{s',l'',l'} G^{m,v,v'}_{l,s,s'} W^{a\,\lambda\lambda'}_{l,L'',l'} \\
& + \frac{1}{2}\sum_{s=\pm1}\sum_{t,t'=-1}^{1}\big[c_{\alpha t'} c^{st}_{\beta}(l,m) + c_{\beta t'} c^{st}_{\alpha}(l,m)\big]\sum_{L\lambda}\sum_{L'\lambda'} A^{av\boldsymbol{k}*}_{L\lambda} A^{av\boldsymbol{k}}_{L'\lambda'} \sum_{L''>0}^{L^{ns}_{max}}\sum_{s,v} G^{v,m'',m'}_{s,l'',l'} G^{v,t',m+t}_{s,1,l+s} V^{a\,\lambda\lambda'}_{l,L'',l'}\Bigg\},
\end{aligned} \tag{G2}$$

where $D^{av\boldsymbol{k}}_{L\lambda}(\alpha,\beta)$ contains the stress variation of the matching coefficients and is expressed as

$$D^{av\boldsymbol{k}}_{lm\lambda}(\alpha,\beta) = \sum_{\boldsymbol{K}} c_{v\boldsymbol{kK}}\, d^{a\boldsymbol{kK}}_{lm\lambda}(\alpha,\beta), \tag{G3}$$

with

$$\begin{pmatrix} d^{a\boldsymbol{kK}}_{lm0}(\alpha,\beta) \\ d^{a\boldsymbol{kK}}_{lm1}(\alpha,\beta) \end{pmatrix} \equiv \frac{1}{\sqrt{\Omega}}\frac{d}{d\epsilon_{\alpha\beta}}\left[\sqrt{\Omega[\underline{\underline{\epsilon}}]}\begin{pmatrix} a^{a\boldsymbol{k}[\underline{\underline{\epsilon}}]\boldsymbol{K}[\underline{\underline{\epsilon}}]}_{lm} \\ b^{a\boldsymbol{k}[\underline{\underline{\epsilon}}]\boldsymbol{K}[\underline{\underline{\epsilon}}]}_{lm} \end{pmatrix}\right]_{\underline{\underline{\epsilon}}=0}, \tag{G4}$$

and integrals $J^{a\lambda\lambda'}_{ll'}$, $V^{a\,\lambda\lambda'}_{l,L'',l'}$, and $W^{a\,\lambda\lambda'}_{l,L'',l'}$ are

$$\begin{aligned}
J^{a\lambda\lambda'}_{ll'} &= \int_0^{R_a} r_a^3 dr_a u^{a\prime}_{l\lambda}(r_a) u^a_{l'\lambda'}(r_a), \\
V^{a\,\lambda\lambda'}_{l,L'',l'} &= \int_0^{R_a} r_a^2 dr_a\, u^a_{l\lambda}(r_a) V^{\mathrm{eff}}_{L''}(r_a) u^a_{l'\lambda'}(r_a), \\
W^{a\,\lambda\lambda'}_{l,L'',l'} &= \int_0^{R_a} r_a^3 dr_a\, u^{a\prime}_{l\lambda}(r_a) V^{\mathrm{eff}}_{L''}(r_a) u^{a\prime}_{l'\lambda'}(r_a), \\
\sigma^{\mathrm{es}}_{\alpha\beta} &= \frac{1}{2}\sum_{\boldsymbol{K}}\sum_{\boldsymbol{K}'\neq 0}\rho^*(\boldsymbol{K})\big[-\delta_{\alpha\beta}V_C(\boldsymbol{K}') + 2\widehat{\boldsymbol{K}}'_{\alpha}\widehat{\boldsymbol{K}}'_{\beta}V_C(\boldsymbol{K}')\big]\Theta(\boldsymbol{K}-\boldsymbol{K}') \\
&\quad - \frac{1}{2\Omega}\sum_a\sum_{t,t'=-1}^{1} c_{\alpha t}c_{\beta t'}\int_0^{R_a} d^3\boldsymbol{r}\,\rho(\boldsymbol{r})V_C(\boldsymbol{r})Y_{1t}(\hat{\boldsymbol{r}})Y_{1t'}(\hat{\boldsymbol{r}}) + \frac{1}{2\Omega}\sum_a Z_a\sum_{t,t'=-1}^{1} c_{\alpha t}c_{\beta t'}V_M(\boldsymbol{\tau}_a)Y_{1t}(\hat{\boldsymbol{\tau}}_a)Y_{1t'}(\hat{\boldsymbol{\tau}}_a),
\end{aligned} \tag{G5}$$

where $\Theta(\boldsymbol{K})$ is the Fourier transform of the step function in the interstitial region;

$$\begin{aligned}
\sigma^{\mathrm{core}}_{\alpha\beta} = -\frac{1}{\Omega}\sum_a\sum_{l,m}\sum_{t,,t'=-1}^{1}\Bigg(& c_{\alpha t}c_{\beta t'}\frac{(-1)^m}{4\pi}G^{-m,t,t'}_{l,1,1}\int_0^{R_a} r_a^3 dr_a\sqrt{4\pi}\,\rho^*_{00}(r_a)\frac{dV_{lm}(r_a)}{dr_a} \\
& + \sum_{s=\pm1}\frac{c^{st}_{\beta}(l,m)c_{\alpha t'} + c^{st}_{\alpha}(l,m)c_{\beta t'}}{2}\frac{(-1)^{t'}}{4\pi}\delta_{1,l+s}\delta_{-t',m+t}\int_0^{R_a} dr_a\sqrt{4\pi}\,r_a^2\rho^*_{00}(r_a)V_{lm}(r_a)\Bigg),
\end{aligned} \tag{G6}$$

$$\sigma^{\mathrm{xc}}_{\alpha\beta} = \frac{\delta_{\alpha\beta}}{\Omega}\int_{\Omega} d^3r\,\rho(\boldsymbol{r})[\epsilon_{\mathrm{xc}}(\rho(\boldsymbol{r})) - \mu_{\mathrm{xc}}(\rho(\boldsymbol{r}))]. \tag{G7}$$

[1] H. G. A. Hellmann, Z. Phys. **85**, 180 (1933).
[2] R. P. Feynman, Phys. Rev. **56**, 340 (1939).
[3] R. Yu, D. Singh, and H. Krakauer, Phys. Rev. B **43**, 6411 (1991).
[4] L. D. Marks, J. Chem. Theory Comput. **17**, 5715 (2021).
[5] O. H. Nielsen and R. M. Martin, Phys. Rev. Lett. **50**, 697 (1983).
[6] O. H. Nielsen and R. M. Martin, Phys. Rev. B **32**, 3780 (1985).
[7] P. Hohenberg and W. Kohn, Phys. Rev. **136**, B864 (1964).
[8] W. Kohn and L. J. Sham, Phys. Rev. **140**, A1133 (1965).
[9] A. Dal Corso and R. Resta, Phys. Rev. B **50**, 4327 (1994).
[10] M. Torrent, F. Jollet, F. Bottin, G. Zrah, and X. Gonze, Comput. Mater. Sci. **42**, 337 (2008).
[11] S. Baroni, P. Giannozzi, and A. Testa, Phys. Rev. Lett. **58**, 1861 (1987).
[12] D. R. Hamann, X. Wu, K. M. Rabe, and D. Vanderbilt, Phys. Rev. B **71**, 035117 (2005).
[13] D. R. Hamann, K. M. Rabe, and D. Vanderbilt, Phys. Rev. B **72**, 033102 (2005).
[14] X. Wu and D. Vanderbilt, and D. R. Hamann, Phys. Rev. B **72**, 035105 (2005).
[15] O. K. Anderson, Phys. Rev. B **12**, 3060 (1975).
[16] D. J. Singh and L. Nordström, *Planewaves, Pseudopotentials, and the LAPW method*, 2nd ed. (Springer, New York, 2006).
[17] T. Thonhauser, C. Ambrosch-Draxl, and D. J. Singh, Solid State Commun. **124**, 275 (2002).
[18] T. Thonhauser, Stress and strain in solids: A formalism for the LAPW method, Ph.D. thesis, Karl-Franzens University Graz, 2001.
[19] N. Nagasako and T. Oguchi, J. Phys. Soc. Jpn. **80**, 024701 (2011).
[20] N. Nagasako and T. Oguchi, J. Phys. Soc. Jpn. **82**, 044701 (2013).
[21] D. A. Klüppelberg, Calculation of stress tensor within the *ab initio* full-potential linearized augmented plane wave method, Diploma thesis, RWTH Aachen, 2011.
[22] J. M. Soler and A. R. Williams, Phys. Rev. B **40**, 1560 (1989).
[23] J. M. Soler and A. R. Williams, Phys. Rev. B **42**, 9728 (1990).
[24] P. Blaha, K. Schwarz, and J. Luitz, WIEN97: A full potential linearized augmented plane wave package for calculating crystal properties, Vienna University of Technology, 1997.
[25] P. Blaha, K. Schwarz, F. Tran, R. Laskowski, G. K. H. Madsen, and L. D. Marks, J. Chem. Phys. **152**, 074101 (2020).
[26] M. Weinert, E. Wimmer, and A. J. Freeman, Phys. Rev. B **26**, 4571 (1982).
[27] M. Weinert, J. Math. Phys. **22**, 2433 (1981).
[28] F. Birch, Phys. Rev. **71**, 809 (1947).
[29] P. E. Blöchl, O. Jepsen, and O. K. Andersen, Phys. Rev. B **49**, 16223 (1994).
[30] M. Weinert and J. W. Davenport, Phys. Rev. B **45**, 13709 (1992).
[31] J. P. Perdew, K. Burke, and M. Ernzerhof, Phys. Rev. Lett. **77**, 3865 (1996).
[32] J. P. Perdew, K. Burke, and M. Ernzerhof, Phys. Rev. Lett. **78**, 1396(E) (1997).
[33] https://www.flapw.de/MaX-5.1/
[34] A. R. Edmonds, *Angular Momentum in Quantum Mechanics* (Princeton University Press, Princeton, NJ, 1985).